

1 **A Central Asia Hydrologic Monitoring Dataset for Food and**
2 **Water Security Applications in Afghanistan**

3 Amy L. McNally^{1,2,3}, Jossy Jacob^{1,4}, Kristi Arsenault^{1,2}, Kimberly Slinski^{1,5}, Daniel P. Sarmiento^{1,2},
4 Andrew Hoell⁶, Shahriar Pervez⁷, James Rowland⁸, Mike Budde⁸, Sujay Kumar¹, Christa Peters-
5 Lidard¹, James P. Verdin³

6

7 1 NASA Goddard Space Flight Center, Greenbelt, MD, 20771, United States

8 2 Science Applications International Corporation Inc., Reston, VA, 20190, United States

9 3 U.S. Agency for International Development, Washington, DC, 20523, United States

10 4 Science Systems and Applications Inc., Lanham, MD, 20706, United States

11 5 University of Maryland Earth Systems Science Interdisciplinary Center, College Park, MD,
12 20740, United States

13 6 National Oceanic and Atmospheric Administration, Physical Science Laboratory, Boulder, CO,
14 80305, United States

15 7 Arctic Slope Regional Corporation Federal Data Solutions, Contractor to U.S. Geological Survey,
16 Earth Resources Observation and Science (EROS) Center, Sioux Falls, SD, 57198, United States

17 8 U.S. Geological Survey, EROS Center, Sioux Falls, South Dakota, 57198, United States

18

19 *Correspondence to:* Amy L. McNally (amy.l.mcnally@nasa.gov)

20 **Abstract**

21
22 From the Hindu Kush Mountains to the Registan desert, Afghanistan is a diverse landscape where
23 droughts, floods, conflict, and economic market accessibility pose challenges for agricultural
24 livelihoods and food security. The ability to remotely monitor environmental conditions is critical to
25 support decision making for humanitarian assistance. The Famine Early Warning Systems Network
26 (FEWS NET) Land Data Assimilation System (FLDAS) global and Central Asia data streams
27 provide information on hydrologic states for routine integrated food security analysis. While
28 developed for a specific project, these data are publicly available and useful for other applications
29 that require hydrologic estimates of the water and energy balance. These two data streams are
30 unique because of their suitability for routine monitoring, as well as a historical record for
31 computing relative indicators of water availability. The global stream is available at ~1 month
32 latency, monthly average outputs on a 10-km grid from 1982-present. The second data stream,
33 Central Asia (30-100 °E, 21-56 °N), at ~1 day latency, provides daily average outputs on a 1-km
34 grid from 2000-present. This paper describes the configuration of the two FLDAS data streams,
35 background on the software modeling framework, selected meteorological inputs and parameters,
36 and results from previous evaluation studies. We also provide additional analysis of precipitation
37 and snow cover over Afghanistan. We conclude with an example of how these data are used in
38 integrated food security analysis. For use in new and innovative studies that will improve
39 understanding of this region, these data are hosted by U.S. Geological Survey data portals and the
40 National Aeronautics and Space Administration (NASA). The Central Asia data described in this
41 manuscript can be accessed via the NASA repository at 10.5067/VQ4CD3Y9YC0R, the global data
42 described in this manuscript can be accessed via the NASA repository at 10.5067/5NHC22T9375G.

43 **1 Introduction**

44 From the Hindu Kush Mountains to the Registan desert, Afghanistan is a diverse landscape where
45 droughts, floods, conflict, and economic market accessibility pose challenges for agricultural
46 livelihoods and food security. The ability to remotely monitor environmental conditions is critical to
47 support decision making for economic development, humanitarian assistance, water resource
48 management, agriculture and more. Environmental datasets can be combined with socio-economic
49 variables and transformed into customized products to support decision making. This is the
50 definition of a ‘climate service’ (Hewitt et al., 2012).

51
52 Hydrologic and land surface datasets are particularly relevant for agriculture and water resources
53 decision making. When these datasets are credible, updated routinely, and made publicly available,
54 the influences of climate variability and climate change can be incorporated into specialized
55 analyses by intermediary users¹. One example of an intermediary user central to this data descriptor
56 is the food security analysts of the Famine Early Warning Systems Network (FEWS NET). FEWS

¹ The WMO defines intermediate (intermediary) users as those who transform climate information into a climate service

57 NET analysts combine environmental information, largely from remote sensing and earth system
58 models, with information on nutrition, livelihoods, markets, and trade to provide decision support to
59 the U.S. Agency for International Development (USAID) Bureau of Humanitarian Assistance.
60 Additional examples and discussion of the production of climate service inputs can be found in the
61 literature (e.g., Vincent et al., 2018; McNally et al., 2019).

62
63 While these data are tailored to specific needs, they are also applicable to other climate services and
64 research e.g., Desert Locusts movement forecasting (Tabar et al., 2021). To that end, this paper
65 describes the FEWS NET Land Data Assimilation System (FLDAS) global and Central Asia data
66 streams. The inputs (e.g., precipitation) and resulting hydrologic estimates (a) provide a 40+ year
67 historical record for contextualizing estimates in terms of departures from average (i.e., anomalies),
68 (b) are low latency (< 1-month) for timely decision support, and (c) are familiar to the food and
69 water security user-community.

70
71 The purpose of this data descriptor is four-fold:

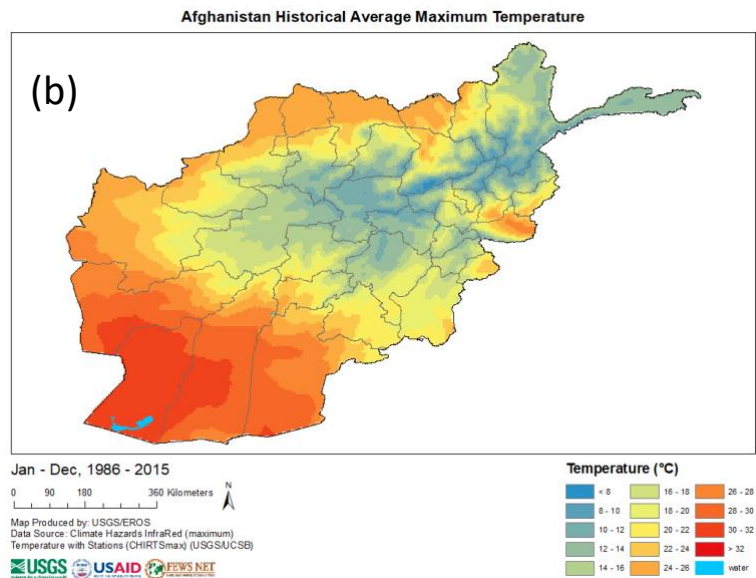
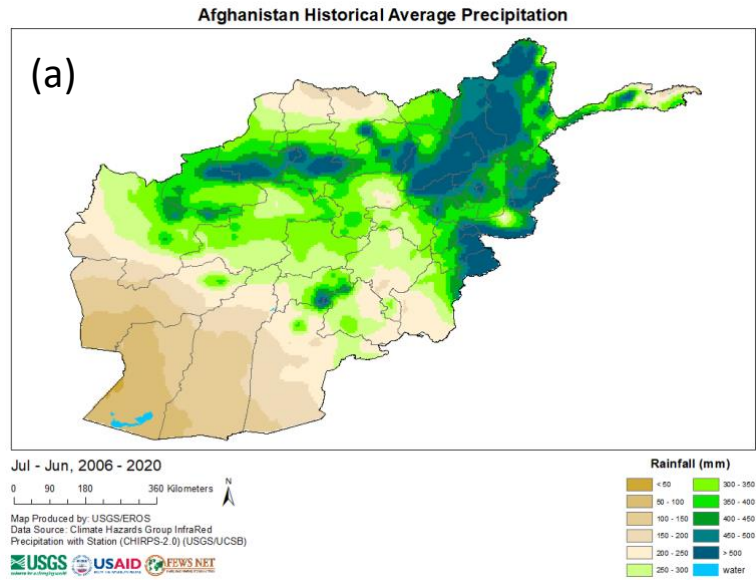
- 72 • to describe the development of the moderate resolution, low latency FLDAS hydrologic
73 monitoring system for Central Asia, specifically Afghanistan
- 74 • to increase awareness of these data resources, which are intended to be a public good,
- 75 • to demonstrate how our methods inform critical investigations that ultimately improve
76 general understanding of water resources in this important region of the world, and
- 77 • to describe a ‘convergence of evidence’ approach to hydrologic monitoring in locations
78 where all sources of information contain some level of uncertainty.

79
80 An outline of this data descriptor is as follows. Section 1.1 provides background on Afghanistan
81 Weather and Climate. Section 1.2 reviews previous studies that have conducted evaluations of the
82 meteorological inputs and hydrologic outputs of Land Data Assimilation Systems in the Central
83 Asia region. Section 2 (Methods) describes the hydrologic modeling system, parameters and
84 meteorological inputs, and model outputs. Section 3 (Results) presents comparisons of precipitation
85 inputs, and comparisons of modeled snow estimates to remotely sensed snow observations. Finally,
86 Section 4 describes an application of these data to the Afghanistan drought of 2018.

87 **1.1 Afghanistan Weather and Climate**

88 Central Asia, a region that includes Afghanistan, is water-scarce, receiving roughly 75% of its
89 annual precipitation during November–April (Oki and Kanae, 2006). In Afghanistan, rainfall is
90 highest in the northeast Hindu Kush Mountains and decreases toward the arid southwest Registan
91 Desert (Fig. 1a). Temperature follows a similar pattern with cooler temperatures in the high
92 elevation, wetter northeast, and warmer temperatures in the south and southwest (Fig. 1b). Regional
93 precipitation is strongly influenced by the El Niño-Southern Oscillation (ENSO). La Niña
94 conditions are associated with below average precipitation (FEWS NET, 2020b) and El Niño
95 conditions are associated with above average precipitation (Barlow et al., 2016; Hoell et al., 2017;
96 Rana et al., 2018; Hoell et al., 2018, 2020; FEWS NET, 2020a). Other factors with an important

97 influence on precipitation include orography, storm tracks, and the Madden–Julian oscillation
 98 (Barlow et al., 2005; Nazemosadat and Ghaedamini, 2010; Hoell et al., 2018). The last several years
 99 have experienced several ENSO events, with recent La Niña events in 2016-17, 2017-18, and 2020-
 100 2022 (NOAA CPC ENSO Cold & Warm Episodes by Season, 2021) that corresponded to droughts
 101 (FEWS NET, 2017b, 2018c, 2021).
 102



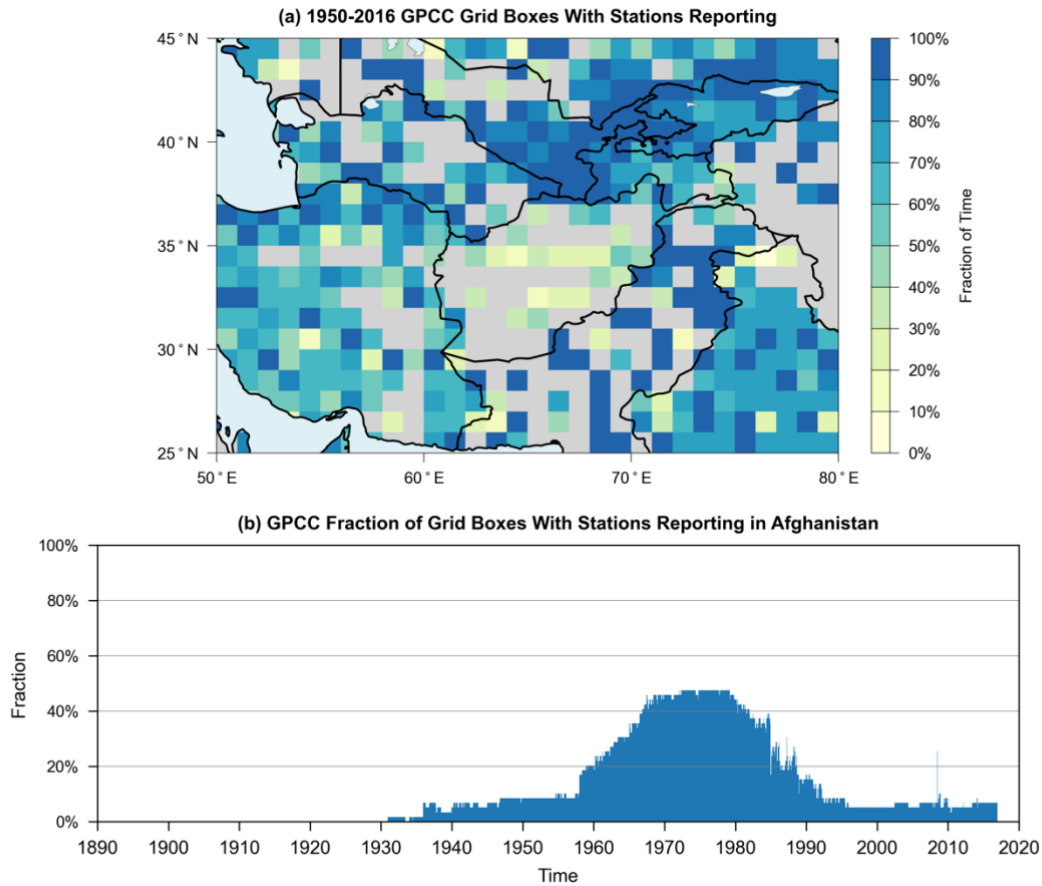
104 Figure 1. (a) Average annual precipitation in Afghanistan from 1991-2020, with overlaid province
105 boundaries. (b) Average maximum monthly temperature from (1986-2015), overlaid with province
106 boundaries. Map source USGS Knowledge Base (USGS Knowledge Base, 2021).
107

108 Despite Afghanistan's semi-arid climate, agriculture is an important sector, contributing 23% of its
109 gross domestic product and employing 44% of the national labor force (CIA World Factbook). High
110 mountain snowpack and snowmelt runoff are important for agricultural water supply. According to
111 FEWS NET (2018b) snowmelt runoff is responsible for "providing over 80% of irrigation water
112 used. The timing and duration of the snowmelt is a key factor in determining the volume of
113 irrigation water and the length of time that it is available, as well as its availability for use in
114 marginal areas that experience [variable] rainfall." Therefore, routine hydrologic monitoring, with a
115 particular emphasis on snow, is critical for tracking agricultural conditions and provides early
116 warning for food insecurity.

117 **1.2 Hydrologic Data Availability and Uncertainty**

118 Remote sensing and models are important inputs to climate services (Qamer et al., 2019). In the
119 Central Asia region, and especially Afghanistan estimates of meteorological inputs, and model
120 parameters have considerable uncertainty due to sparse in situ environmental observations. To
121 address these challenges, the NASA High Mountain Asia project (<https://www.himat.org/>) has
122 broadly aimed to explore the driving changes in hydrology as well as model validation and data
123 assimilation, and water budget processes from the Himalayas in the south and east to the Hindu
124 Kush in the west. These efforts and other studies of satellite derived rainfall informed the
125 configuration and interpretation of the FLDAS Central Asia and global data streams.
126

127 The primary challenge to producing and evaluating hydrologic estimates is that sparse in situ
128 precipitation observations lead to uncertainty in gridded, satellite-based precipitation estimates.
129 Precipitation station observations are used for (a) bias correction of satellite estimates and (b)
130 validation of gridded products. In terms of gridded dataset development, Hoell et al. (2015) describe
131 how lack of station observations and complex topography in Afghanistan, Iraq, and Pakistan makes
132 this issue particularly problematic. Barlow et al. (2016) also highlight the station availability across
133 the region and how that influences uncertainties in the Global Precipitation Climatology Center
134 (GPCC) version 6 (Schneider et al., 2017) dataset over Central Asia (Fig. 2a) and specifically
135 Afghanistan over time (Fig. 2b).
136



137
 138 Figure 2. (a) Station data availability underlying the GPCC version 6 dataset, for the 1950–2016
 139 period, on the 0.5° -resolution grid over Central Asia. (b) Fraction of gridcells with Number of
 140 stations used as input to the GPCC rainfall dataset in Afghanistan from 1932-2016.

141
 142 In the absence of abundant in situ observations, one approach for remote sensing and model
 143 evaluation is to compare multiple input datasets and evaluate the water balance. Independent
 144 observations from the different components of the water balance (e.g., evapotranspiration, soil
 145 moisture, streamflow) help constrain estimates. We provide some background here and refer readers
 146 and data users to literature from the NASA High Mountain Asia project, specifically Yoon et al.
 147 (2019) and Ghatak et al. (2018), who explored similar configurations to the FLDAS system. This
 148 background allows the reader to appreciate the uncertainties in inputs, outputs and derived products
 149 and climate services over Afghanistan and the broader Central Asia region.

150
 151 Meteorological forcing is known to be the primary source of uncertainty in land surface model
 152 simulations (Kato and Rodell, 2007). Thus, its evaluation is important to understand the quality of
 153 model inputs and outputs. For this reason, Ghatak et al. (2018) compare four unique precipitation
 154 data sources: daily Climate Hazards center Infrared Precipitation with Stations (CHIRPS) (Funk et

155 al., 2015), NOAA’s Global Data Assimilation System (GDAS) (Derber et al., 1991), and two
156 estimates from NASA’s Modern Era Reanalysis for Research and Applications version 2 (MERRA-
157 2) (Gelaro et al., 2017). They find that annual CHIRPS and GDAS precipitation estimates had
158 similar bias and root mean squared error over Afghanistan with respect to APHRODITE (Asian
159 Precipitation Highly Resolved Observational Data Integration Toward Evaluation) rain-gauge
160 derived product (Yatagai et al., 2012). CHIRPS had a higher correlation with APHRODITE. Ghatak
161 et al. (2018) further evaluated the quality of rainfall inputs based on the performance of
162 evapotranspiration and other derived outputs. The authors caution that gridded precipitation
163 estimates that have in situ inputs, like CHIRPS, may systematically underestimate precipitation in
164 mountainous regions. We keep this consideration in mind when interpreting differences between
165 FLDAS global and Central Asia data streams.

166
167 Yoon et al. (2019) compare precipitation estimates from 10 different products including
168 APHRODITE, CHIRPS, GDAS, and MERRA-2, across a broad region of High Asia, including a
169 portion of Afghanistan. They find that all datasets generally capture the spatial pattern of rainfall
170 and that the products tend to agree more at high elevations, where it is unlikely there are station
171 observations. Like Ghatak et al. (2018), they found CHIRPS and APHRODITE to have a lower
172 average precipitation than GDAS, attributable to the incorporation of sparse gauge data.

173
174 In addition to precipitation, other meteorological inputs are important for accurate hydrologic
175 estimates. Yoon et al. (2019) conducted an intercomparison of near surface air temperature
176 estimates from three model analysis products (European Centre for Medium-Range Weather
177 Forecasts (ECMWF; Molteni et al., 1996), GDAS, and MERRA-2). They noted a statistically
178 significant upward trends in GDAS and ECMWF temperature, as well as consistently higher
179 temperatures in MERRA-2. We see the same pattern when averaging across Afghanistan. Yoon et
180 al. (2019) conclude that improvements in the meteorological boundary conditions would be needed
181 to reduce the uncertainty in the terrestrial budget estimates. These sentiments are echoed in Qamer
182 et al. (2019).

183
184 Despite known uncertainties, Schiemann et al. (2008) find that gridded precipitation estimates can
185 qualitatively identify large scale spatial distribution of precipitation, seasonal cycles, and interannual
186 variability (i.e., wet and dry years) across Central Asia. Long-term estimates of rainfall from
187 satellite derived products, as well as derived historical time series from hydrologic modeling, can be
188 used as a baseline of “observations,” from which we can have a sense of relative conditions, i.e.,
189 anomalies and variability. When this historical record is harmonized with a routine monitoring
190 system, current conditions can be placed in historical context. Anomaly-based representation of
191 hydrologic extremes can provide confidence in modeled estimates that have the potential to
192 influence agricultural, water resources and food security outcomes. For these reasons one of the
193 requirements for FLDAS input is that there is a sufficiently long historical record for
194 contextualizing estimates in terms of anomalies.

195

196 From a climate services perspective, the reliance on the representation of relatively wet and dry
197 conditions, as well as a “convergence of evidence” approach, provide useable information despite
198 the above-mentioned uncertainties. A convergence of evidence approach that draws on (quasi-
199 independent sources of information is useful to understand actual conditions. For convergence of
200 Earth observations, hydrologic models can generate ensembles of historical, current, or future
201 estimates of snow, streamflow, soil moisture, and evapotranspiration, which can then be compared
202 to satellite derived estimates of surface water (e.g., McNally et al., 2019), soil moisture (e.g.,
203 McNally et al., 2016), vegetation conditions and evapotranspiration (e.g., Jung et al., 2019; Pervez
204 et al., 2021), snow cover (e.g., Arsenault et al., 2014), in situ streamflow (e.g. Jung et al., 2017) and
205 others. Hydrologic estimates can also be compared to outcomes in crop production (e.g., (e.g.,
206 McNally et al., 2015; Davenport et al., 2019; Shukla et al., 2020), and nutrition, health, and food
207 security (e.g., Grace and Davenport, 2021) to provide a qualitative understanding of both hydrologic
208 model performance and conditions on the ground. In this paper we provide an example for 2018
209 where drought conditions were associated with crisis levels of acute food insecurity over most of
210 Afghanistan (FEWS NET, 2018c).

211
212 To summarize, our experience and the literature have characterized uncertainties in available
213 meteorological forcing for the region. GDAS, CHIRPS, and MERRA-2 were chosen for the FLDAS
214 system based on our project requirements of (a) a sufficiently long historical record for
215 contextualizing estimates in terms of anomalies (b) low latency (< 1-month) for timely decision
216 support, (c) familiar to the FEWS NET user-community, and (d) prior evaluation by our team and
217 the broader community. We note here and describe in more detail later that the Integrated Multi-
218 satellite Retrievals for the Global Precipitation Mission (IMERG), a NASA precipitation product
219 (Huffman et al., 2020) also meets these requirements, since version 6 which was released in 2019
220 (after these studies and initial FLDAS configuration). We will a describe IMERG, GDAS, and
221 MERRA-2 comparison in the Results (Section 3).

222 **2 Methods**

223 **2.1 Land Surface Modeling System & Parameters**

224 A land surface model (LSM) can provide spatially and temporally continuous information about the
225 water and energy budgets of the land surface. This information is useful for food and water security
226 applications in places where in situ measurements of rainfall, soil moisture, snow and runoff are
227 sparse. This is particularly relevant in mountainous places like Afghanistan where heterogeneous
228 geography limits the representativeness of sparse in situ measurements. The FLDAS (McNally et
229 al., 2017) utilizes the NASA’s Land Information System Framework (LISF), which is composed of
230 a pre-processor, the Land surface Data Toolkit (Arsenault et al., 2018), the Land Information
231 System (Kumar et al., 2006; Peters-Lidard et al., 2007), and the Land Verification Toolkit (Kumar
232 et al., 2012). In this data descriptor we describe the two configurations of the FLDAS data streams
233 used for Central Asia food and water security applications. It uses the Noah 3.6 LSM (Chen et al.,

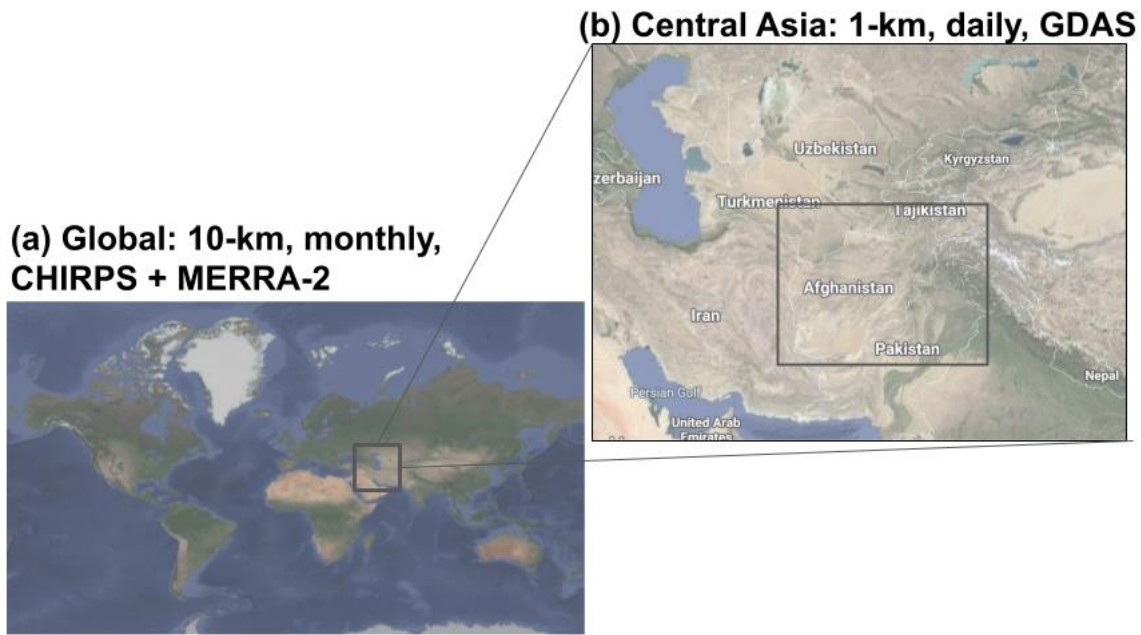
234 1996; Ek et al., 2003) for the two data streams (Fig. 3 and Table 1). The first data stream is global,
235 at ~1 month latency, and provides monthly average outputs on a 10-km grid from 1982-present. The
236 second data stream centered on Central Asia, ~1 day latency, provides daily average outputs at 1-km
237 from 2001-present.

238

239 One important feature, added by the NASA LISF software development team, is the radiation
240 correction described in Kumar et al. (2013), which improves the representation of snow dynamics
241 with respect to slope and aspect corrections on the downward solar radiation field. Another
242 noteworthy feature is the method of the Central Asia data stream restart (i.e., annual initialization
243 based on climatology), which was developed to address an issue of excessive inter-annual snow
244 accumulation found in the Noah LSM. First, a nine-year spin-up of the system was performed to
245 produce stable snow and soil moisture conditions. Next, the resulting model states were compared
246 with the Moderate Resolution Imaging Spectroradiometer (MODIS) Maximum Snow Extent data
247 originally computed by NOAA National Operational Hydrologic Remote Sensing Center (Greg Fall,
248 NOAA Operational Data Center, written communication., 2014). Then, the model-estimated
249 conditions were adjusted to produce a climatological model state for 1 October that is used to
250 initialize each year. This approach ensures that the ‘water year,’ beginning 1 October, is initialized
251 with a reasonable initial amount of snowpack. While this method does effectively manage excessive
252 inter-annual modeled snow accumulation, the user should be aware that using the climatological
253 model state will persist for ~1-2 months in the water and energy balance of the LSM until they are
254 superseded by “observed” meteorological inputs for the current water year. Preliminary work
255 indicates that this issue will be resolved in future updates. In contrast, the global data stream does
256 not use this 1 October initialization procedure.

257 Although the two data stream specifications are largely the same, there are some differences related
258 to the input forcings, parameters and specifications (Table 1) and model spin-up procedures.

259



260
 261 Figure 3. The FEWS NET Land Data Assimilation System (FLDAS) domains for (a) the global data
 262 stream at 10-km spatial resolution and ~1 month latency for monthly averaged hydrologic estimates
 263 and (b) the Central Asia data stream at 1-km spatial resolution and ~1 day latency for daily averaged
 264 hydrologic estimates.

265
 266 Table 1. FEWS NET Land Data Assimilation System (FLDAS) specifications for (A) global data
 267 stream, 10-km monthly with CHIRPS+MERRA-2; and (B) Central Asia data stream, 1-km, daily
 268 with GDAS.

	Global	Central Asia
Spatial Extent	179.95°W- 179.95°E, 59.95°S-89.95°N	30-100°E, 21-56°N
Landmask	Generated from MODIS using LISF-LDT, with MOD44w mask applied post-processing.	MOD44w (Carroll et al., 2017)
Landcover	IGBP landcover	IGBP landcover
Elevation	Shuttle Radar Topography Mission SRTM (NASA JPL, 2013)	SRTM
Albedo	National Centers for Environmental Prediction (NCEP) albedo (Csiszar	NCEP albedo & MODIS-based Max Snow Albedo

	and Gutman, 1999) & MODIS-based Max Snow Albedo (Barlage et al., 2005)	
Vegetation Parameters	NCEP greenness fraction (Gutman and Ignatov, 1998)	NCEP greenness fraction
Non-Precipitation Meteorological Inputs	MERRA-2	GDAS
Soil Texture	Food and Agricultural Organization (FAO) soil texture & properties (Reynolds et al., 2000)	FAO soil texture & properties
Precipitation Inputs	CHIRPS daily precipitation, downscaled to 6-hourly with LDT	GDAS 3-hourly precipitation
Specifications	Noah 3.6.1	Noah 3.6.1
Map Projection	Geographic Latitude-Longitude	Geographic Latitude-Longitude
Software Version	7.2	7.3
Spatial Resolution	10-km	1-km
Temporal Coverage	1982-01-01 to present	2000-10-01 to present
Model Timestep	15-min timestep	30-min timestep
Met. Forcing Heights	2-m Air Temperature (Tair), 10-m Wind	2-m Tair, 10-m Wind
Soil layers (meters)	0-0.1; 0.1-0.4; 0.4-1.0; 1-2	0-0.1; 0.1-0.4; 0.4-1.0; 1-2
Features	radiation correction	radiation correction

269

270 The parameters and specifications listed in Table 1 are largely default settings defined by the Noah
271 LSM community (NCAR Research Applications Library, 2021). Ongoing research aims to identify
272 where model output performance can be improved with parameter updates. Evaluating parameter
273 updates had similar challenges as evaluating input forcing described in Section 1.2: without reliable
274 reference data it is difficult to determine a “best” input. For example, we have explored changing
275 soil parameters from FAO to International Soil Reference and Information Centre (ISRIC) SoilGrids
276 database (Hengl et al., 2017). This change did not result in improvements in streamflow statistics in
277 southern Africa, nor in soil moisture anomalies’ ability to represent drought events. We expect
278 similar results in Afghanistan where, e.g., streamflow will be sensitive to a change in soil
279 parameters and the lack of referenced data to evaluate if there is an improvement. Moreover, our

280 model runs at 0.1 and 0.01 degrees may not fully exploit the added value of the 250m soil grids as
281 noted in Ellenburg et al. (2021) for a LISF application in East Africa.

282 Vegetation parameters are also potential sources of improvement whose importance to LDAS
283 hydrologic estimates has been highlighted (e.g., Miller et al., 2006). We have found the NCEP
284 estimates of green vegetation fraction (GVF) to be sufficient for this configuration of Noah 3.6. We
285 found that a time series of GVF derived from the Normalized Difference Vegetation Index (NDVI)
286 did not improve representation of droughts in eastern Africa. However, future FLDAS global and
287 Central Asia versions can be run with Noah-Multi parameterization (Noah-MP) (Niu et al., 2011)
288 which has multiple vegetation options and relies on either Leaf Area Index rather or GVF. This
289 model update is expected to open possibilities for choice of datasets to meet our application needs
290 and potentially improve representation of the water balance.

291 **2.2 Meteorological Forcing Inputs**

292 As previously discussed, precipitation is a critical input to land surface models. The lower-latency
293 Central Asia data stream is a daily product, forced with GDAS (Derber et al., 1991) 3-hourly
294 precipitation, which is available from 2001 to present at <1-day latency. This dataset was chosen
295 because of its latency. The global data stream is driven by the daily CHIRPS product (Funk et al.,
296 2015), which is available from 1981 to present at ~ 5-day latency for CHIRPS Preliminary and ~1.5-
297 month latency for CHIRPS Final. The CHIRPS products were chosen as inputs because of their
298 proven performance in the literature, which has made it the “gold standard” for food and water
299 security monitoring by organizations like FEWS NET, the World Food Program, and others who
300 need up-to-date estimates and a 40+ year historical record. As mentioned earlier, lack of rainfall
301 stations for bias correction of satellite-derived estimates and evaluation poses a major challenge.
302 However, we find that the GDAS rainfall product and the CHIRPS rainfall product are adequate for
303 routine monitoring and, along with additional sources of remote sensed information, are important
304 for convergence of evidence when making a best estimate at land surface states and fluxes.

305
306 Before the daily CHIRPS rainfall data can be used as input to the FLDAS models, the daily
307 precipitation is pre-processed to a sub-daily timestep, using the LDT component of the LISF
308 software. LDT temporally disaggregates the daily CHIRPS rainfall using an approach similar to the
309 North American LDAS precipitation temporal downscaling (Cosgrove et al., 2003). For this
310 approach, we use a finer timescale MERRA-2 precipitation timescale as a reference dataset to
311 represent an accurate diurnal cycle. We note that this step in our methodology facilitates the solving
312 of FLDAS water and energy balances at a sub-daily timestep. However, for Central Asia we do not
313 have sufficient reference data available to assess the importance of sub-daily precipitation
314 distribution, as was demonstrated by Sarmiento et al. (2021) for the United States where adequate
315 reference data are available. For spatial downscaling, coarser scale meteorological forcings are
316 spatially disaggregated to the output resolution (0.01, and 0.1 degree for Central Asia and global,
317 respectively) in the LISF using bilinear interpolation.

318 The FLDAS models require additional meteorological inputs, including air temperature, humidity,
319 radiation, and wind. The lower-latency Central Asia data stream uses GDAS 3-hourly
320 meteorological inputs available from 2001-present at <1-day latency. For a longer historical record,
321 the global data stream uses MERRA-2 (Gelaro et al., 2017) (1979-present) 1-hourly products with a
322 two-week latency. Over the Afghanistan domain GDAS temperature has an upward trend, whereas
323 MERRA-2 is consistently warmer before 2010. We find that GDAS and MERRA-2 temperature
324 estimates are of similar magnitude during 2011-2020. Similar results were noted by Yoon et al.
325 (2019) who found an upward trend in GDAS temperature, as well as consistently higher
326 temperatures in MERRA-2 across a broad High Asia domain.

327 **2.3 Model Evaluation Statistics and Comparison Data**

328 In addition to guidance from previous studies (Section 1.2), we assessed the quality of our modeling
329 outputs by conducting comparisons between (1) FLDAS satellite rainfall inputs and other satellite
330 precipitation estimates, and (2) model estimated snow cover fraction and satellite derived snow
331 cover fraction estimates.
332

333 For the precipitation analysis, we compare CHIRPS and GDAS inputs to the Integrated Multi-
334 satellite Retrievals for the Global Precipitation Mission (IMERG), a NASA precipitation product
335 that integrates passive microwave and infrared satellite data with surface station observations
336 (Huffman et al., 2020). The IMERG Final Run precipitation product, available at ~ 2-month latency
337 (thus not suitable for our monitoring applications) has been used in numerous verification studies,
338 including studies over Africa (Dezfuli et al., 2017), South America (Gadelha et al., 2019; Manz et
339 al., 2017), and the mid-Atlantic region of the United States (Tan et al., 2016). These studies
340 demonstrated that IMERG Final Run was able to capture large spatial patterns and seasonal and
341 interannual patterns of rainfall. However, fewer studies have explored the performance of the lower
342 latency IMERG Late Run (doi: 10.5067/GPM/IMERGDL/DAY/06) product that we use here.
343 Kirshbaum et al. (2016) include a qualitative comparison for CHIRPS Final and IMERG Late Run
344 for the Southern Africa start-of-season 2015. IMERG Late Run appears to perform similarly to the
345 1.5-month latency CHIRPS Final and outperform the 1-day latency NOAA Rainfall Estimate
346 version 2 (RFE2) product (Xie and Arkin, 1996). Differences in the daily rainfall distribution
347 patterns between IMERG Final Run and CHIRPS Final have also been shown to affect the resulting
348 hydrological modeled output in simulations done using the NASA LISF (Sarmiento et al., 2021).
349

350 For the snow cover fraction (SCF) analysis, we compare the global and Central Asia data streams
351 with the MODIS daily SCF product, MOD10A1 Collection 6 (Hall and Riggs, 2016). MOD10A1
352 data are available at 500-m spatial resolution from February 2000 to the present. SCF is generated
353 using the Normalized Difference Snow Index (NDSI) and additional filters to reduce error and flag
354 uncertainty. Routine qualitative comparisons, which can be viewed on the NASA LISF FEWS NET
355 project website, generally show agreement between the model and MODIS SCF, as well as
356 occurrence of cloud cover (<https://ldas.gsfc.nasa.gov/fldas/models/central-asia>). Following
357 Arsenault et al. (2014), we aggregated pixels to 0.01 degree to reduce error related to sensor viewing

358 angles and gridding artifacts. For this analysis, using MODIS SCF as “truth,” we determined True
359 Positives (TP), True Negatives (TN), False Negatives (FN) and False Positives (FP). We then
360 computed probability of detection (POD) where $POD = (TP / (TP + FN))$ and False Alarm Rate
361 (FAR) where $FAR = (FP / (FP + TN))$. We computed these for the total area of Afghanistan (60-76E,
362 28-39N), as well as by basin (Fig. 4). This paper does not compare modeled snow water equivalent
363 (SWE) to independent snow observations because, as noted by Yoon et al. (2019), direct evaluation
364 of snow mass and SWE) is difficult over Central Asia due to poor coverage of accurate snow
365 observations. We follow the Yoon et al. (2019) recommendation to conduct quantitative SCF
366 comparisons and provide qualitative SWE analysis in Applications, Section 4.

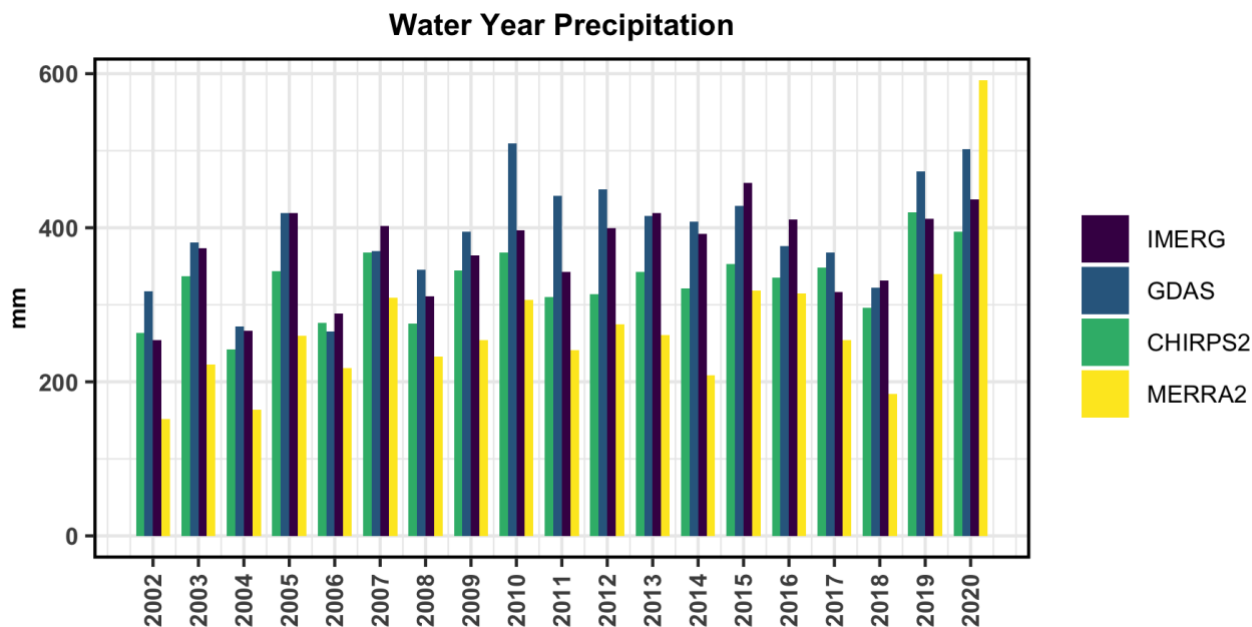
367
368 In addition to rainfall and snow comparisons, we conducted monthly pixel-wise comparison of
369 Central Asia and the global run’s estimates of evapotranspiration (ET) and soil moisture versus
370 Operational Simplified Surface Energy Balance (SSEBop, (Senay et al., 2013)). ET and Soil
371 Moisture Active Passive (SMAP) Level 3 (Entekhabi et al., 2010, 2016) using the Normalized
372 Information Contribution (NIC) metric following Sarmiento et al., (2021). The analysis was
373 performed for the period 2016-2021 to match the SMAP record. The NIC metric first computes
374 anomaly correlations between the model runs and the reference dataset and then computes the
375 difference between the performance of each model run using a scale of -1 to +1 to highlight if the
376 global or Central Asia data stream performs better with respect to the reference. To make the
377 comparisons, the reference datasets (SMAP and SSEBop) were re-gridded to match the grid spacing
378 and locations of the experiment model outputs.

379 **3 Results**

380 **3.1 Gridded Rainfall Comparison**

381 We have two data streams for Central Asia applications with different precipitation inputs: 1) the
382 global data stream with CHIRPS precipitation at 10-km spatial resolution provides a long-term
383 consistent data record; and 2) the Central Asia data stream with GDAS precipitation at 1-km
384 provides near real time, finer spatial resolution updates. These two data streams have their
385 respective errors and allow data users to apply a convergence of evidence approach for food and
386 water security applications. This section presents a comparison of the GDAS, and CHIRPS
387 precipitation inputs used for the Central Asia and global data streams, respectively. We also include
388 IMERG Late Run for comparison as a high quality, low latency product. Future work may
389 incorporate the IMERG Late Run precipitation inputs into FLDAS simulations. We also include
390 MERRA-2 precipitation for comparison. Pair-wise correlations are shown in Table 2. CHIRPS
391 Final, IMERG Late Run and GDAS ($R \geq 0.90$) are well correlated in terms of average daily
392 precipitation (mm/day) at the monthly and annual (i.e., water year) timestep. MERRA-2 correlations
393 with these datasets are lower at the monthly ($0.75 \leq R \leq 0.81$) and water year ($0.64 \leq R \leq 0.69$)
394 timesteps. Fig. 4 shows the time series of the precipitation products for their overlapping period of
395 record (2001-2020), which illustrates how they vary in time, and shows some general patterns in
396 terms of relative precipitation in mm: GDAS (blue) and IMERG Late Run (purple) tend to have the

397 highest precipitation totals, CHIRPS (green) has lower precipitation but is higher than MERRA-2
 398 (yellow) which tends to have the lowest precipitation, until 2019 when it is notably higher than the
 399 other products.



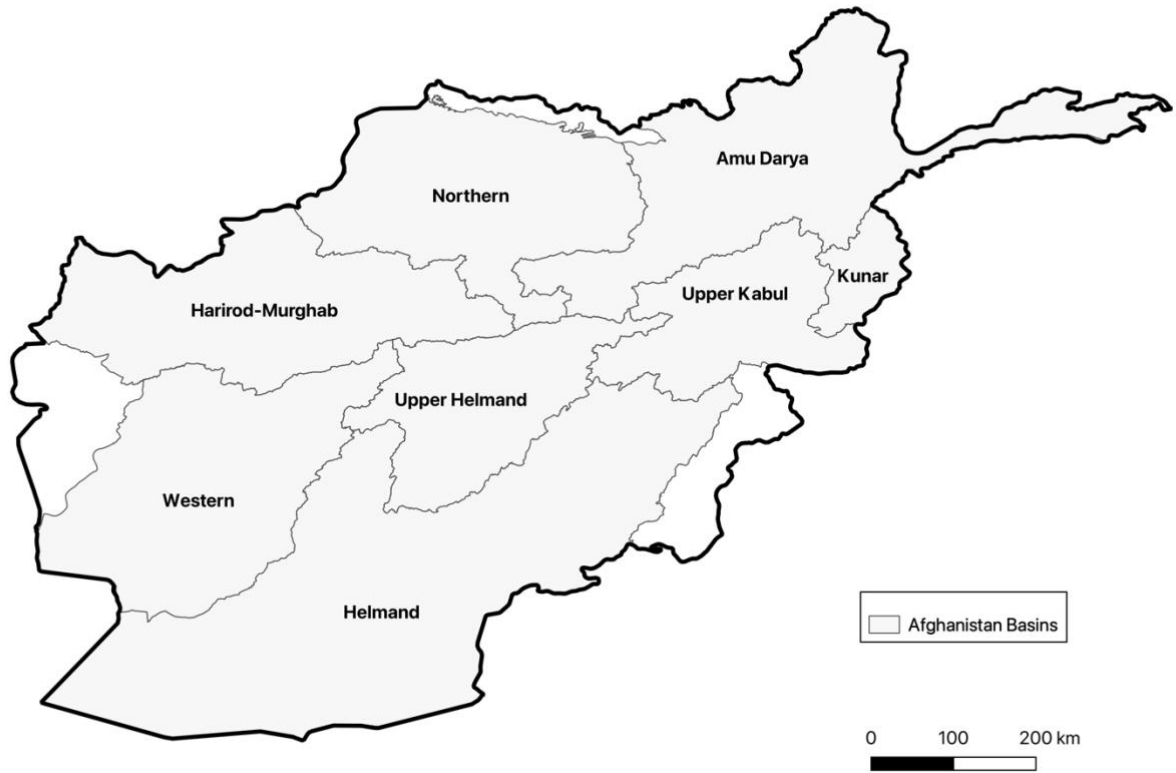
400
 401
 402 Figure 4. Afghanistan water year precipitation for CHIRPS, GDAS, IMERG Late Run, and
 403 MERRA-2.

404
 405 Table 2. Afghanistan spatial average Spearman Rank Correlation (R) of monthly (water year)
 406 precipitation 2001-2020

	GDAS	CHIRPS Final	IMERG Late Run
GDAS	x	-	-
CHIRPS Final	0.91 (0.92)	x	-
IMERG Late Run	0.91 (0.89)	0.92 (0.90)	x
MERRA-2	0.75 (0.64)	0.78 (0.68)	0.81(0.69)

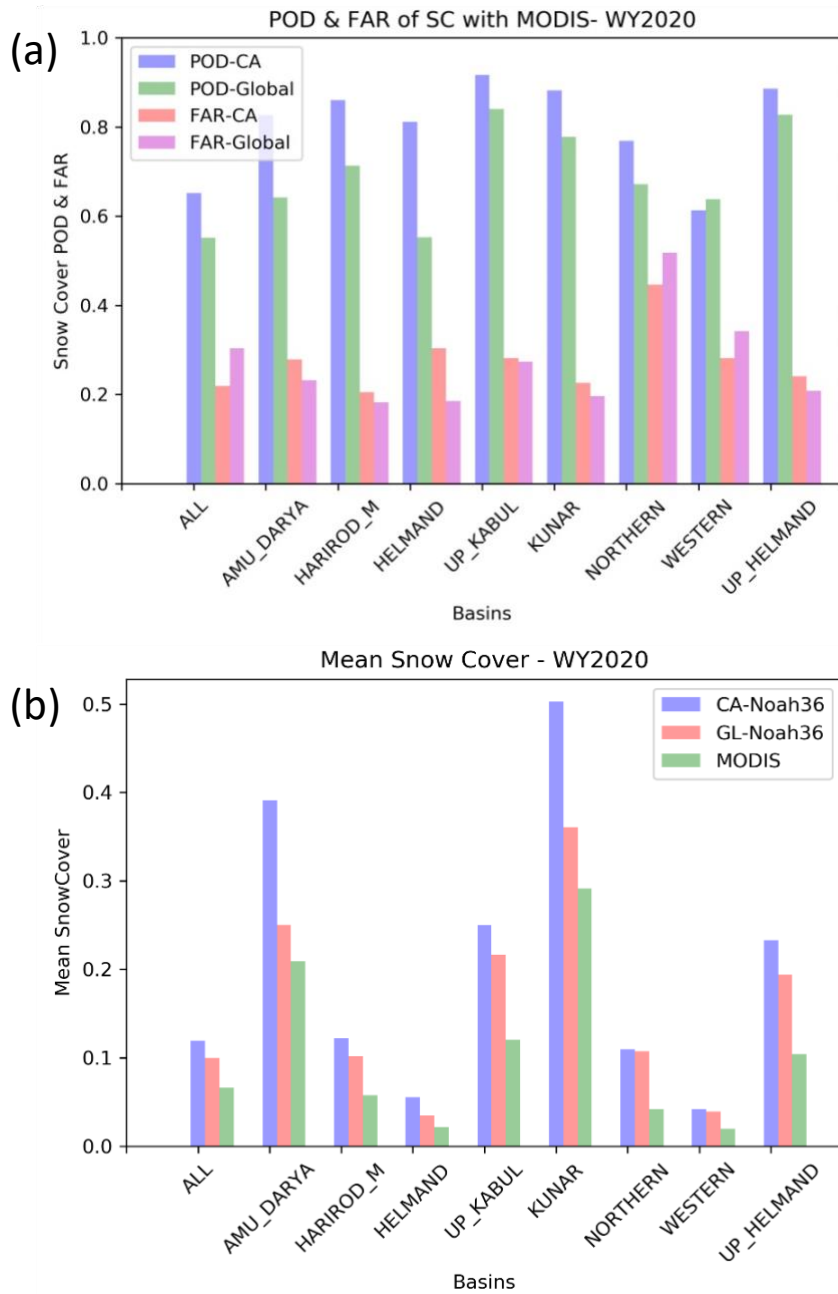
407
 408 **3.2 Remotely Sensed and Modeled Snow comparisons**

409 The estimation of snow is important for Afghanistan and Central Asia because it is a critical
 410 contributor to water resources and irrigated agriculture. We compared average SCF (Fig. 6a), POD,
 411 and FAR statistics (Fig. 6b) relative to MODIS SCF over eight hydrologic basins in Afghanistan.
 412



413
414
415

Figure 5. Hydrologic basins used in the analysis of categorical statistics for snow covered fraction.



416
 417 Figure 6. (a) Mean snow cover fraction for the entire area and by hydrologic basin for MODIS
 418 Snow Cover Fraction (SCF), Central Asia (CA) and global (GL) data streams for water year 2020.
 419 (b) Probability of Detection (POD) of snow presence, and False Alarm Rate (FAR) for the Central
 420 Asia (CA) and global data streams relative to the MODIS SCF for water year 2020.
 421

422 Overall, both model runs estimate greater average SCF than the MODIS SCF product. The Central
423 Asia data stream has consistently higher average snow cover for all basins compared to MODIS
424 SCF estimates and the global data stream. Perhaps not surprisingly that the Central Asia data stream
425 performs consistently better in POD (by basin = ~80%) except for the Western Basin. Similarly, the
426 FAR of the Central Asia data stream is higher where POD is higher except for the Northern Basin.
427 The difference in statistics may be related to the different forcing inputs or the higher spatial
428 resolution of the Central Asia data stream. Kumar et al. (2013) note that higher spatial resolution
429 was important for snow dominated basins.

430
431 In addition to precipitation and snow cover comparisons we conducted comparisons with remotely
432 sensed soil moisture and ET (not shown). We found that in general, GDAS derived estimates of ET
433 consistently performed better over Afghanistan in terms of pixel-wise anomaly correlation and NIC
434 with SSEBop ET. Meanwhile, neither modeled estimate of soil moisture consistently outperformed
435 the other with respect to SMAP. The ET results lend some support to the quality of the Central Asia
436 data stream estimates. However, the lack of signal in the soil moisture comparisons suggests that
437 more careful analysis of the model and remote sensing errors is required before drawing conclusions
438 regarding which data stream is “best.”

439 **3.3 Discussion of results compared to previous studies**

440 Despite the lack of ground-based observations, our analysis shows that the remotely sensed
441 estimates and the models have good correspondence with other sources of evidence in terms of
442 seasonal timing and performance. This provides analysts with confidence when using the FLDAS
443 snow estimates, in tandem with other sources, as an input to food security assessments. Our
444 approach is supported by other studies that have explored the challenges of evaluating hydrologic
445 estimates over the region (Immerzeel et al., 2015; Ghatak et al., 2018; Yoon et al., 2019; Qamer et
446 al., 2019).

447
448 Yoon et al. (2019) show that their LSM ensembles of SCF have an average POD of 72% and FAR
449 of 36%, which is within the range of our POD and FAR statistics (60-80% POD; 20-40% FAR)
450 compared to MODIS SCF. The categorical statistics indicate that Central Asia (GDAS) tends to
451 have both a higher probability of detection and false alarm rate, indicating higher averages than
452 MODIS SCF and global (CHIRPS).

453
454 With respect to the soil moisture and ET comparisons, we found that the Central Asia data stream
455 estimates of ET were better correlated with SSEBop ET, but neither data stream was consistently
456 better correlated with SMAP. These differences could be a function of non-precipitation differences,
457 or higher spatial resolution. Ghatak et al. (2018) also found that the choice of reference dataset (with
458 its own characteristics and errors) was an important factor.
459

460 In general, given the lack of clarity on “best” FLDAS data stream, the convergence of evidence
 461 approach allows us to consult both data streams, leveraging the longer time series of CHIRPS and
 462 the lower latency of GDAS.

463 3.4 Limitations and Future Developments

464 Given the need for multiple data streams for convergence of evidence, we have summarized the pros
 465 and cons of the Central Asia and global data streams in Table 3.

466
 467 Table 3. Pros and cons of the two data streams

	Central Asia: Noah 3.6 with GDAS (2000-present)	Global: Noah 3.6 with CHIRPS+MERRA-2 (1982-present)
Pros	1-km	less computationally intensive
	1-day latency, daily timestep	longer time record
	Snow estimates available in USGS Early Warning eXplorer https://earlywarning.usgs.gov/fews/ewx/	CHIRPS & MERRA-2 forcing spatial resolution does not change over time (stable climatology)
		Water and Energy balance available in NASA GIOVANNI https://giovanni.gsfc.nasa.gov/giovanni/ ; Google Earth Engine https://developers.google.com/earth-engine/datasets/tags/fldas ; Climate Engine https://climateengine.com/
Cons	more computationally intensive	lower resolution (10-km)
	shorter time record	~30-day latency
	GDAS forcing resolution changes over time (unstable climatology) (NOAA NCEP https://www.emc.ncep.noaa.gov/gmb/STATS/html/model_changes.html)	not publicly available at daily timestep
	large data volume, difficult to move	

468

469 IMERG version 6 was released in 2019 and includes rainfall estimates processed back to 2000. Prior
 470 to this change we had found encouraging results when comparing the onset of rainy season using
 471 both IMERG Late Run and CHIRPS (Kirschbaum et al., 2016). However, at that time the period of
 472 record was a limitation for computing anomalies. We now have an adequate period of record, and
 473 IMERG Late Run is planned to be part of the upcoming FLDAS global and FLDAS Central Asia
 474 releases. We are also encouraged by the quality of IMERG at the daily timestep when compared to
 475 CHIRPS over the United States where accurate reference data are available (Sarmiento et al., 2021).

476
 477 In addition to IMERG other promising rainfall datasets are in development. Ma et al. (2020) have
 478 developed the AIMERG dataset that combines IMERG Final Run with the APHRODITE rain-gauge
 479 derived product (Yatagai et al., 2012). Another promising dataset is CHIMES (Funk et al., 2022), a
 480 blend of CHIRPS and IMERG, whose developers have been exploring the strengths and limitations
 481 of these two datasets and their fusion to produce an optimal product.

482
 483 With respect to other FLDAS developments, FLDAS global and Central Asia are planned to be
 484 transition to Noah-MP. This will allow for improved representation of snowpack and groundwater.
 485 This will also necessitate the use of different parameters, e.g., leaf area index, as well as the
 486 potential to explore different parameter sets like ISRIC soils. In the meantime, multi-forcing and
 487 multi-model ensembles, and convergence of evidence with other remotely sensed data and field
 488 reports, are a viable approach for providing hydrologic estimates for various applications.

489 **4 Applications**

490 These data from global and Central Asia data streams are routinely used in several FEWS NET
 491 information products listed in Table 4. NOAA’s Climate Prediction Center (CPC) International
 492 Desks provide a weekly briefing on the past week’s weather conditions and 1– 2-week forecasts for
 493 FEWS NET regions of interest, including Central Asia. There is also a monthly FEWS NET
 494 Seasonal Monitor and a monthly Seasonal Forecast Review for which these data provide
 495 information on the current state of the snowpack, soil moisture, and runoff. These “observed
 496 conditions" can then be qualitatively combined with forecasts 1 week to many months in the future
 497 to assess potential hydro-meteorological hazards. To demonstrate the role of these data in the early
 498 warning process, at different points in the season, we provide an example of the 2017-2018 wet
 499 season in Afghanistan during a La Niña event that contributed to drought.

500
 501 Table 4. Routine Applications of FLDAS Central Asia’s Afghanistan hydrologic data.

Routine application of these data	Weblink to updates	Notes
FEWS NET Global Weather Hazards	https://fews.net/global/global-weather-hazards/	shapefiles https://ftp.cpc.ncep.noaa.gov/fews/weather_hazards/

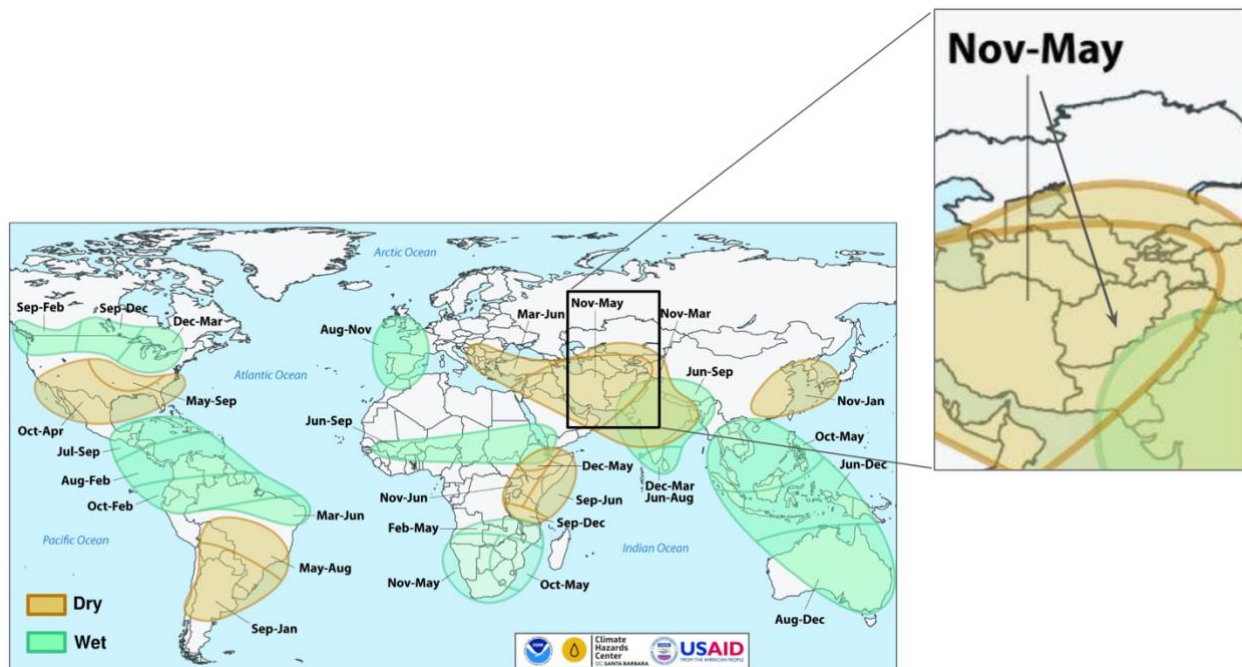
Summary produced by NOAA CPC	https://www.cpc.ncep.noaa.gov/products/international/index.shtml	
Seasonal Monitor	https://earlywarning.usgs.gov/fews/afghanistan/seasonal-monitor	Updated near the middle of each month from October - May, the wet season.
FEWS NET Food Security Outlook Brief	https://fews.net/central-asia/afghanistan	Information on snow or other hydrology included if applicable
Crop Monitor for Early Warning	https://cropmonitor.org/index.php/cmreports/early-warning-report/	Information on early warning and crop conditions

502

503 4.1 Snow Monitoring & Seasonal Outlooks

504 As previously mentioned, and as shown in Fig. 7, Afghanistan and the broader region is strongly
505 influenced by La Niña, which tends to increase the likelihood of below average precipitation.
506 Depending on this and antecedent conditions there is an increased likelihood of below average
507 snowpack, reduce springtime streamflow and flood risk, reduce summer irrigation water
508 availability, and crop yield losses.

509



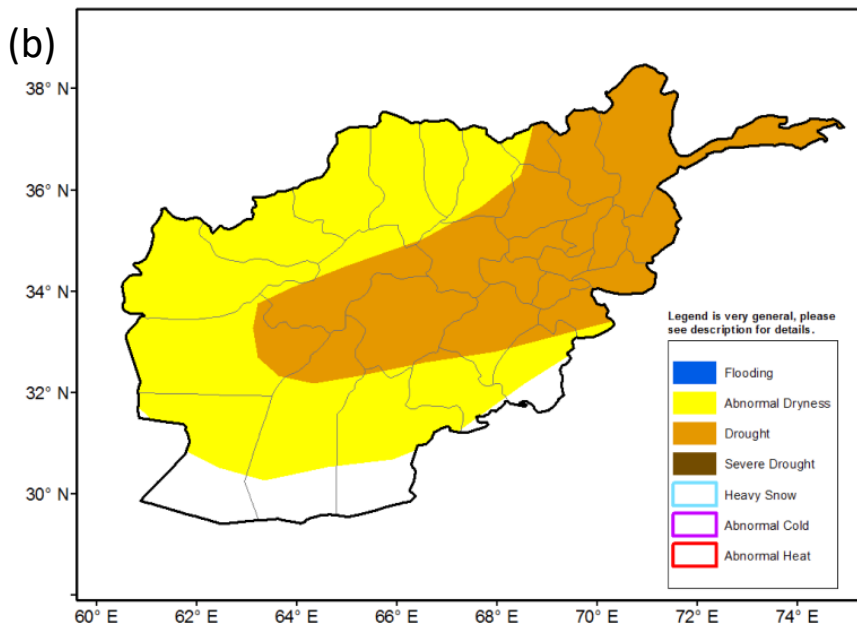
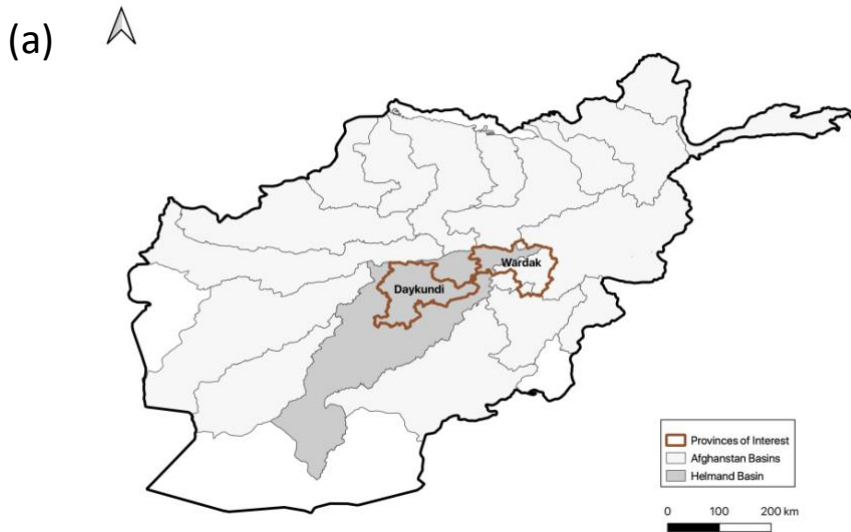
510

511 Figure 7. Timing of wet and dry conditions related to La Niña. Increased likelihood of dry
512 conditions from November-May for Afghanistan during La Niña events.

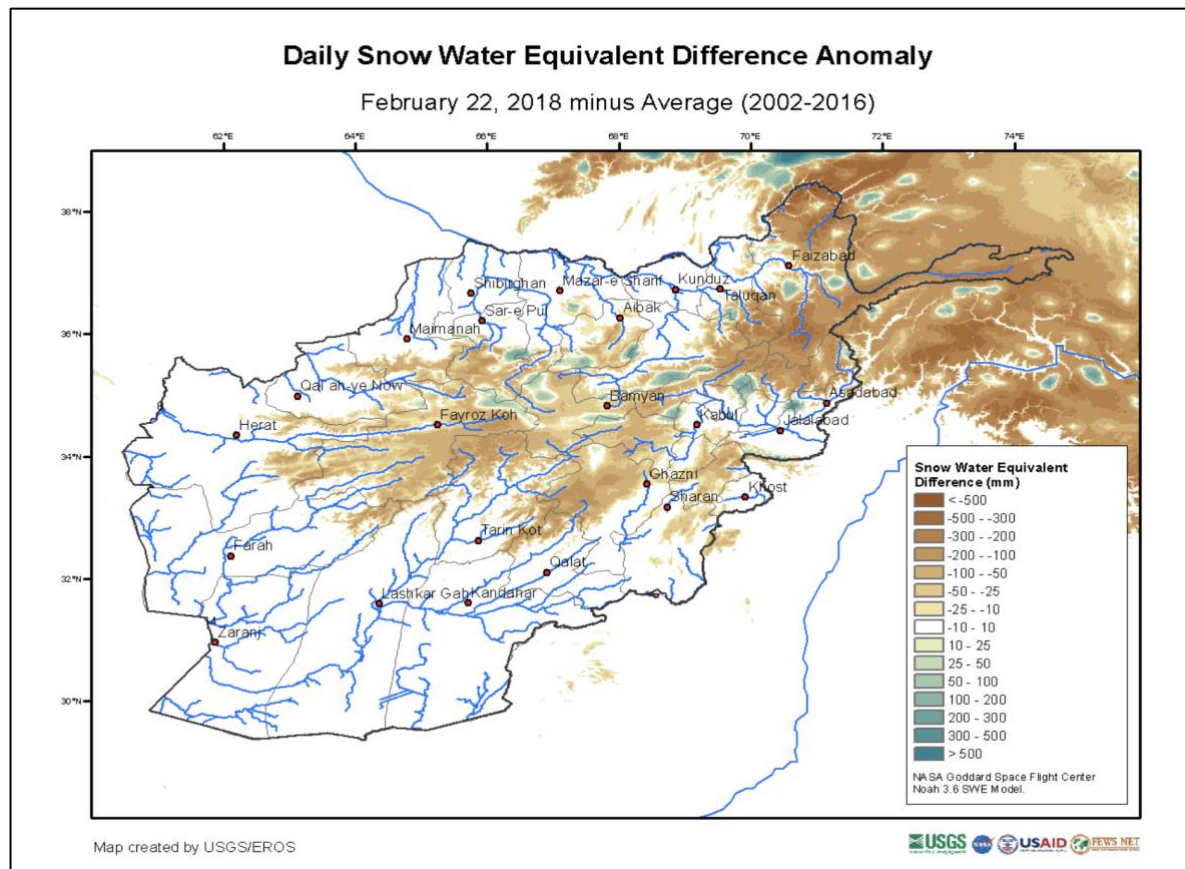
513
514 A La Niña Watch was issued by NOAA in September 2017 (NOAA, 2017). The FEWS NET
515 October 2017 Food Security Outlook (FEWS NET, 2017a) stated that La Niña conditions were
516 expected throughout the northern hemisphere fall and winter and that below-average precipitation
517 was likely over much of Central Asia, including Afghanistan, during the 2017-2018 wet season.
518 With the expectation of below average precipitation coupled with above average temperatures,
519 FEWS NET anticipated that snowpack would most likely be below average. In the context of food
520 security outcomes, it was assumed that areas planted with winter wheat were likely to be less than
521 usual, reducing land preparation activities and associated demand for labor. Two provinces of
522 particular concern were Daykundi and Wardak (Fig. 8a brown borders), both located in the
523 Helmand River Basin (Fig. 8a; gray shading). Precipitation deficits in these provinces would lead to
524 poor rangeland resources and pasture availability and would likely result in decreased livestock
525 productivity and milk production through May. However, given that October was the start of the wet
526 season, there remained a large spread of possible outcomes: spatial and temporal rainfall
527 distributions, and snowpack totals necessitating routine updates to assumptions.

528
529 Monitoring continued during the wet season, tracking observations from remote sensing, models,
530 and field reports as well as forecasts across timescales. This information was used to regularly
531 update expectations of end of season outcomes. Using the FLDAS Central Asia data stream, a
532 December 21, 2017, NOAA CPC Weather Hazards Brief reported that parts of northern and central
533 Afghanistan remained atypically snow free, and north-eastern high elevation areas exhibited SWE
534 deficits. SWE is a commonly used measurement of the amount of liquid water contained within the
535 snowpack, and an indicator of the amount of water that will be released from the snowpack when it
536 melts. By January 17, 2018, an abnormal dryness polygon was placed over northeastern Afghanistan
537 and the central highlands, based on below-average SWE values from the FLDAS Central Asia
538 estimates. Abnormal dryness is defined for an area that has registered cumulative 4-week
539 precipitation and soil moisture ranking less than the 30th percentile, with a Standardized
540 Precipitation Index (SPI) of 0.4 standard deviation below the average. In addition, it is required that
541 forecasts indicate below-average precipitation (less than 80% of normal) for that area during the 1-
542 week outlook period. By late February 2018, precipitation deficits and related SWE (Fig. 9)
543 increased and met the criteria for “drought” (Fig. 8b). Drought is defined as an area that has
544 previously been defined as “Abnormal Dryness” and has continued to register seasonal precipitation
545 and soil moisture deficits since the beginning of the rainfall season. Specifically, an eight-week
546 cumulative precipitation, soil moisture, and runoff below the 20th percentile rank, and an SPI of 0.8
547 standard deviation below the average are classification guidelines.

548



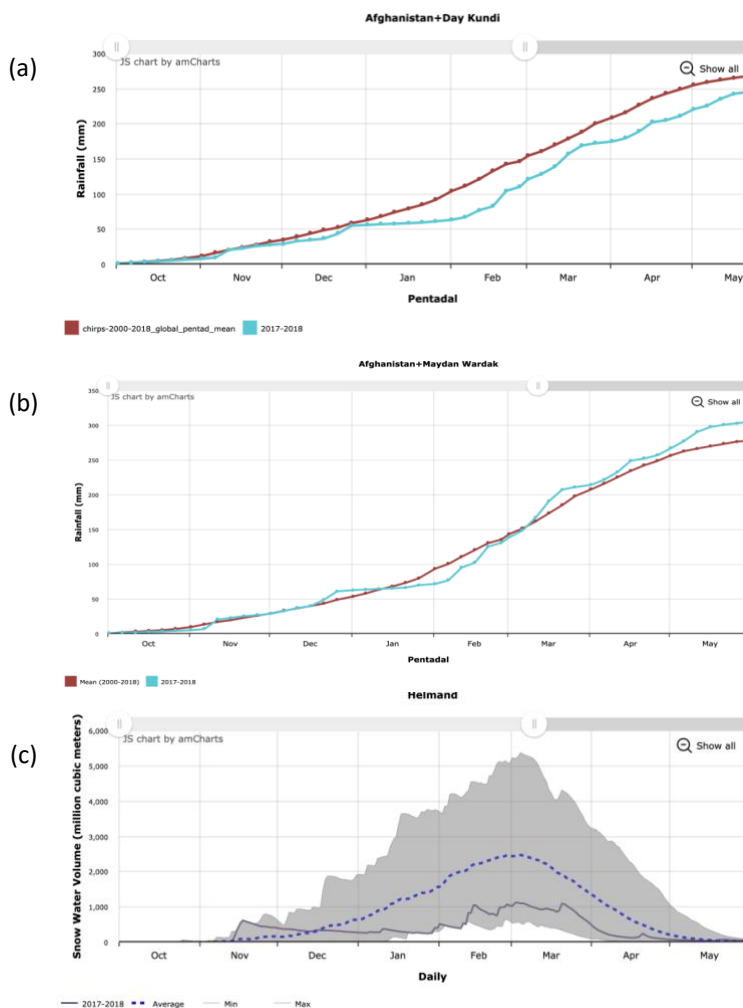
549
 550 Figure 8. (a) Map showing hydrological basins, with Helmand Basin in darker gray and location of
 551 Daykundi and Wardak provinces (outlined in red) where food security conditions were of particular
 552 concern, (b) NOAA CPC Afghanistan Hazards Report for February 22-28, 2018 (CPC NOAA,
 553 2018) showing widespread abnormal dryness and drought, defined by 90-day precipitation deficits
 554 and extremely low snow water equivalent.
 555



556
557 Figure 9. FLDAS Central Asia snow water equivalent (SWE) estimates for February 22, 2018.
558 SWE deficits of 300-mm were widespread at this time.
559

560 The February 2018 Food Security Outlook (FEWS NET, 2018b) provided the following updates,
561 based on the CPC Hazards Reports and Seasonal Monitors: “Snow accumulation and cumulative
562 precipitation were well below average for the season through February 2018, with some basins at or
563 near record low snowpack, with data since 2002....These factors will likely have an adverse impact
564 on staple production in marginal irrigated areas and in many rainfed areas. [Moreover, with]
565 forecasts for above-average temperatures during the spring and summer, rangeland conditions are
566 expected to be poor during the period of analysis through September 2018. This could have an
567 adverse impact on pastoralists and agro-pastoralists, particularly in areas where livestock
568 movements are limited by conflict.” The Crop Monitor for Early Warning reports for February and
569 March 2018 (GEOGLAM, 2018a, b) also cited reduced snowpack in Afghanistan and the negative
570 impacts on winter wheat crops as well as irrigation water availability in the Spring. The story was
571 also highlighted in NASA Earth Observatory March 2018 “Record Low Snowpack in Afghanistan”
572 (NASA Earth Observatory, 2018).
573

574 The USGS Early Warning eXplorer (EWX) (Shukla et al., 2021) allows analysts to look at maps
 575 and time series for a variety of variables and specific provinces and river basins. Plots from EWX in
 576 Fig. 10 show below average precipitation for provinces in the Helmand Basin for January and
 577 February. CHIRPS cumulative rainfall for 2017-18 versus the 18-year average for Day Kundi (a.k.a.
 578 Daykundi) Province showed near average conditions until December. From January, cumulative
 579 rainfall remained below the 2000-2018 average throughout the rest of the season ending in May; the
 580 same pattern occurred in nearby Uruzgan Province. In neighboring Maydan Wardak (a.k.a Wardak)
 581 Province, below average conditions were experienced in January and February, but cumulative
 582 rainfall recovered in March to remain slightly above average. Day Kundi (Fig. 10b) and Wardak
 583 (Fig. 10c) are provinces located in the upper reaches of the Helmand Basin. Fig. 10c shows SWE
 584 averaged across the entire Helmand basin. The gray shading indicates the range of the minimum and
 585 maximum values, and the dashed blue line is the average. Initial snow conditions start above
 586 average until December, after which SWE deficits are near record low values through the beginning
 587 of February, and then persist at below-average levels.



588

589 Figure 10. (a) CHIRPS cumulative rainfall for 2017-18 versus average conditions for Daykundi
590 Province. (b) CHIRPS cumulative rainfall for 2017-18 versus average conditions for Maydan
591 Wardak Province (c) Helmand Basin SWE from the FLDAS Central Asia data stream. The grey
592 shading indicates the range of the minimum and maximum values, dashed blue line is the average,
593 and black line is 2017-18. Figures from USGS EWX (<https://earlywarning.usgs.gov/fews/ewx/>).

594
595 By the end of the season in April 2018, FEWS NET (2018c) concluded that “below-average
596 precipitation throughout most of the country during the October 2017 – May 2018 wet season has
597 led to very low snowpack ...Low irrigation water availability is likely to have an adverse impact on
598 yields for winter wheat and other ...barley, maize, and others.. particularly in downstream areas in
599 regions with limited rainfall. ...The poor performance of the wet season and above average
600 temperatures... exacerbated dry rangeland conditions in many areas, particularly in ...Sari Pul, [and
601 surrounding] ...provinces. Pastoralists and agropastoralists in these areas will likely attempt to
602 migrate to areas with better pasture and water availability or sell livestock at below-average prices.”
603 At the same time, UNICEF (2018) reported in April 2018 that among “the [drought] affected
604 provinces, Baghis, Bamyán, Daykundi, Ghor, Helmand, ... and Uruzgan are of critical priority for
605 nutrition and water, sanitation and hygiene assistance.”

606
607 Several months after a season has ended, and harvest is complete, more statistics become available
608 for further verification of the drought outcomes. The FEWS NET October 2018 Food Security
609 Outlook (2018a) reported that the 2017-18 drought had significant negative impacts on rainfed
610 wheat production and livestock pasture and body conditions across the country. Reporting statistics
611 from the Afghanistan Ministry of Agriculture, Irrigation, and Livestock, the total wheat production
612 for the 2017-18 season was about 20% below average, where irrigated agriculture performed about
613 average. However, rainfed agricultural production was only about 50% of average, most severely
614 affecting households in Badakhshan, Badhis, and Daykundi provinces. In these locations dry
615 conditions, conflict, poor incomes, and depleted assets were expected to continue to face emergency
616 food insecurity through May 2019.

617 **5. Data Availability**

618 The Central Asia data described in this manuscript can be accessed at the NASA GES DISC
619 repository under data doi 10.5067/VQ4CD3Y9YC0R. The data citation is the following:

620
621 Jacob, Jossy and Slinski, Kimberly (NASA/GSFC/HSL) (2021), FLDAS Noah Land Surface Model
622 L4 Central Asia Daily 0.01 x 0.01 degree, Greenbelt, MD, USA, Goddard Earth Sciences Data and
623 Information Services Center (GES DISC) 10.5067/VQ4CD3Y9YC0R

624
625 The global data described in this manuscript can be accessed at the NASA GES DISC repository
626 under data doi 10.5067/5NHC22T9375G. The data citation is the following:

627

628 McNally, Amy. NASA/GSFC/HSL (2018), FLDAS Noah Land Surface Model L4 Global Monthly
629 0.1 x 0.1 degree (MERRA-2 and CHIRPS), Greenbelt, MD, USA, Goddard Earth Sciences Data and
630 Information Services Center (GES DISC), 10.5067/5NHC22T9375G

631
632 Currently the USGS EROS Center provides images from these data:
633 <https://earlywarning.usgs.gov/fews/search/Asia/Central%20Asia>, as well as an interactive data
634 viewer, the USGS EWX (<https://earlywarning.usgs.gov/fews/ewx/>).

635 **6. Code availability**

636 The NASA Land Information System Framework (LISF) is publicly available and an open-source
637 software. The software and technical support are available at <https://github.com/NASA-LIS/LISF>.

638 **7. Conclusion**

639 This paper describes a comprehensive hydrologic analysis system for food security monitoring in
640 Central Asia, with analysis focusing on Afghanistan. While these data are tailored to specific needs,
641 they are also applicable to other climate services and research. Our intent is to provide the reader
642 with information regarding the configuration and specification of both the current global and Central
643 Asia data streams. These data are publicly available and available at near-real time for food security
644 decision support. Note that, as an on-going initiative, FLDAS model version and parameters are
645 routinely updated, and the user should consult the version updates provided by the NASA Goddard
646 Earth Science Data and Information Services Center (GES DISC) data provider and documentation
647 on USGS Early Warning website. For example, efforts are currently underway to upgrade to the
648 Noah-MP (Niu et al., 2011) land surface model, which requires some changes in parameters for
649 snow, glaciers and groundwater. This, and future changes, can be informed by the strengths and
650 weaknesses of the data stream configurations that we have discussed in this paper.

651
652 This paper also provides model-model and model-remote sensing comparisons as well as a review
653 of other research that highlights the challenges of quantitative evaluation of models and remote
654 sensing in this region. A key challenge to hydrologic modeling is the considerable uncertainty in the
655 meteorological forcing available for this region, particularly precipitation. Advancements in remote
656 sensing and modeling should help reduce these uncertainties. In addition, the current land surface
657 modeling reflects natural conditions, i.e., they do not include representation of anthropogenic effects
658 such as human water abstractions (e.g., dams for flood control or irrigation, water diversions,
659 groundwater pumping) or land application of abstracted water (i.e., irrigation). These factors affect
660 estimates of runoff, soil moisture, evapotranspiration, and sensible heat flux (land surface
661 temperatures) in irrigated areas. Therefore, it is important to be aware of the limitations and
662 combine with other products (e.g., NDVI or Actual Evapotranspiration (ETa) in irrigated areas)
663 when exploring water and energy balance. Even with improvements to meteorological forcing and
664 modeling parameterizations, errors will remain. Therefore, the ‘convergence of evidence’ approach

665 is beneficial and would be important when assessing hydro-meteorological hazards and associated
666 risks to food and water security. By making the data publicly available the broader food security and
667 water resources communities will be able to provide insights that can lead to improvements in our
668 understanding of the water and energy balance that can ultimately lead to improvements to food and
669 water security decision support systems.

670

671 **8. Author contribution**

672 JJ runs the code, updates websites, and archives routinely. DS maintains LISF code used in paper,
673 JJ, KA, DS, SP conducted model evaluation AM, KS, CPL, SK contributed to design of evaluation.
674 JR, MB, SP manage the data for USGS distribution. AH, JV provide feedback on data quality and
675 interpretation. AM prepared the manuscript with contributions from all co-authors.

676 **9. Acknowledgements**

677 The authors wish to acknowledge the original version of the Central Asia snow modeling with LIS6
678 performed at NOAA National Operational Hydrologic Remote Sensing Center by Greg Fall and
679 Logan Karsten. USGS work was performed under U.S. Agency for International Development
680 (USAID), Bureau of Humanitarian Assistance (BHA) PAPA AID-FFP-T-17-00003 and USGS
681 contract 140G0119C0001. Any use of trade, firm, or product names is for descriptive purposes only
682 and does not imply endorsement by the U.S. Government. KS, AH, DS, JJ, NASA work was
683 performed under USAID BHA PAPA AID-FFP-T-17-00001. KS, AH acknowledge support from
684 the NASA Harvest Consortium (NASA Applied Sciences Grant No. 80NSSC17K0625). Computing
685 resources have been provided by NASA's Center for Climate Simulation (NCCS). Distribution of
686 data from the Goddard Earth Sciences Data and Information Services Center (GES DISC) is funded
687 by NASA's Science Mission Directorate (SMD). We thank NOAA CPC International Desk for use
688 of figures, and the NASA Land Information System Team for software support and development.
689 The authors also thank the USGS reviewer for comments that improved the quality of the
690 manuscript.

691 **10. References**

692 Arsenault, K. R., Houser, P. R., and De Lannoy, G. J. M.: Evaluation of the MODIS snow cover
693 fraction product: Satellite-based snow cover fraction evaluation., *Hydrol. Process.*, 28, 980–998,
694 <https://doi.org/10.1002/hyp.9636>, 2014.

695 Arsenault, K. R., Kumar, S. V., Geiger, J. V., Wang, S., Kemp, E., Mocko, D. M., Beaudoin, H.
696 K., Getirana, A., Navari, M., Li, B., Jacob, J., Wegiel, J., and Peters-Lidard, C. D.: The Land
697 Surface Data Toolkit (LDT v7.2) - A Data Fusion Environment for Land Data Assimilation
698 Systems, *Geosci. Model Dev.*, 11, <https://doi.org/10.5194/gmd-11-3605-2018>, 2018.

699 Barlage, M., Zeng, X., Wei, H., and Mitchell, K. E.: A global 0.05° maximum albedo dataset of
700 snow-covered land based on MODIS observations: Maximum Albedo of Snow-covered, *Geophys.*
701 *Res. Lett.*, 32, <https://doi.org/10.1029/2005GL022881>, 2005.

702 Barlow, M., Wheeler, M., Lyon, B., and Cullen, H.: Modulation of Daily Precipitation over
703 Southwest Asia by the Madden–Julian Oscillation, *Monthly Weather Review*, 133, 3579–3594,
704 <https://doi.org/10.1175/MWR3026.1>, 2005.

705 Barlow, M., Zaitchik, B., Paz, S., Black, E., Evans, J., and Hoell, A.: A Review of Drought in the
706 Middle East and Southwest Asia, *Journal of Climate*, 29, 8547–8574, <https://doi.org/10.1175/JCLI->
707 [D-13-00692.1](https://doi.org/10.1175/JCLI-D-13-00692.1), 2016.

708 Carroll, M., DiMiceli, C., Wooten, M., Hubbard, A., Sohlberg, R., and Townshend, J.: MOD44W
709 MODIS/Terra Land Water Mask Derived from MODIS and SRTM L3 Global 250m SIN Grid V006
710 [Data set]. NASA EOSDIS Land Processes DAAC., 2017.

711 Chen, F., Mitchell, K., Schaake, J., Xue, Y., Pan, H.-L., Koren, V., Duan, Q. Y., Ek, M., and Betts,
712 A.: Modeling of land surface evaporation by four schemes and comparison with FIFE observations,
713 *J. Geophys. Res.*, 101, 7251–7268, <https://doi.org/10.1029/95JD02165>, 1996.

714 CIA World Factbook: <https://www.cia.gov/the-world-factbook/countries/afghanistan/#introduction>.

715 Cosgrove, B. A., Lohmann, D., Mitchell, K. E., Houser, P. R., Wood, E. F., Schaake, J. C., Robock,
716 A., Marshall, C., Sheffield, J., Duan, Q., Luo, L., Higgins, R. W., Pinker, R. T., Tarpley, J. D., and
717 Meng, J.: Real-time and retrospective forcing in the North American Land Data Assimilation
718 System (NLDAS) project, *J. Geophys. Res.*, 108, 2002JD003118,
719 <https://doi.org/10.1029/2002JD003118>, 2003.

720 CPC NOAA: Weather Hazards Outlook of Afghanistan and Central Asia for the Period of February
721 22 - 28, 2018, 2018.

722 Csiszar, I. and Gutman, G.: Mapping global land surface albedo from NOAA AVHRR, 104, 6215–
723 6228, <https://doi.org/10.1029/1998JD200090>, 1999.

724 Davenport, F. M., Harrison, L., Shukla, S., Husak, G., Funk, C., and McNally, A.: Using out-of-
725 sample yield forecast experiments to evaluate which earth observation products best indicate end of
726 season maize yields, *Environ. Res. Lett.*, 14, 124095, <https://doi.org/10.1088/1748-9326/ab5ccd>,
727 2019.

728 Derber, J. C., Parrish, D. F., and Lord, S. J.: The New Global Operational Analysis System at the
729 National Meteorological Center, *Weather and Forecasting*, 6, 538–547,
730 [https://doi.org/10.1175/1520-0434\(1991\)006<0538:TNGOAS>2.0.CO;2](https://doi.org/10.1175/1520-0434(1991)006<0538:TNGOAS>2.0.CO;2), 1991.

- 731 Dezfuli, A. K., Ichoku, C. M., Huffman, G. J., Mohr, K. I., Selker, J. S., van de Giesen, N.,
732 Hochreutener, R., and Annor, F. O.: Validation of IMERG Precipitation in Africa, *Journal of*
733 *Hydrometeorology*, 18, 2817–2825, <https://doi.org/10.1175/JHM-D-17-0139.1>, 2017.
- 734 Ek, M. B., Mitchell, K. E., Lin, Y., Rogers, E., Grunmann, P., Koren, V., Gayno, G., and Tarpley, J.
735 D.: Implementation of Noah land surface model advances in the National Centers for Environmental
736 Prediction operational mesoscale Eta model, *JGR: Atmospheres*, 108,
737 <https://doi.org/10.1029/2002JD003296>, 2003.
- 738 Ellenburg, W. L., Mishra, V., Roberts, J. B., Limaye, A. S., Case, J. L., Blankenship, C. B., and
739 Cressman, K.: Detecting Desert Locust Breeding Grounds: A Satellite-Assisted Modeling
740 Approach, *Remote Sensing*, 13, 1276, <https://doi.org/10.3390/rs13071276>, 2021.
- 741 Entekhabi, D., Njoku, E. G., O’Neill, P. E., Kellogg, K. H., Crow, W. T., Edelstein, W. N., Entin, J.
742 K., Goodman, S. D., Jackson, T. J., Johnson, J., Kimball, J., Piepmeier, J. R., Koster, R. D., Martin,
743 N., McDonald, K. C., Moghaddam, M., Moran, S., Reichle, R., Shi, J. C., Spencer, M. W.,
744 Thurman, S. W., Tsang, L., and Zyl, J. V.: The Soil Moisture Active Passive (SMAP) Mission, 98,
745 704–716, <https://doi.org/10.1109/JPROC.2010.2043918>, 2010.
- 746 Entekhabi, D., Das, N., Njoku, E. G., Johnson, J., and Shi, J. C.: SMAP L3 Radar/Radiometer
747 Global Daily 9 km EASE-Grid Soil Moisture, Version 3, NASA National Snow and Ice Data Center
748 DAAC [preprint], <https://doi.org/10.5067/7KKNQ5UURM2W>, 2016.
- 749 FEWS NET: Afghanistan Food Security Outlook October 2017-May 2018 Conflict, dry spells, and
750 weak labor opportunities will lead to deterioration in outcomes during 2018 lean season, 2017a.
- 751 FEWS NET: Update on performance of the October 2016 – May 2017 wet season, 2017b.
- 752 FEWS NET: Afghanistan Food Security Outlook: Emergency assistance needs are atypically high
753 through the lean season across the country, FEWS NET, 2018a.
- 754 FEWS NET: Afghanistan Food Security Outlook February to September 2018: Low snow
755 accumulation and dry soil conditions likely to impact 2018 staple production, 2018b.
- 756 FEWS NET: Afghanistan Food Security Outlook Update April 2018: Poor rangeland conditions and
757 below-average water availability will limit seasonal improvements, 2018c.
- 758 FEWS NET: El Niño and Precipitation, FEWS NET, [https://fews.net/el-ni%C3%B1o-and-](https://fews.net/el-ni%C3%B1o-and-precipitation)
759 [precipitation](https://fews.net/el-ni%C3%B1o-and-precipitation), 2020a.
- 760 FEWS NET: La Niña and Precipitation, FEWS NET, [https://fews.net/la-ni%C3%B1a-and-](https://fews.net/la-ni%C3%B1a-and-precipitation)
761 [precipitation](https://fews.net/la-ni%C3%B1a-and-precipitation), 2020b.

- 762 FEWS NET: Afghanistan Food Security Outlook February to September 2021: Below-average
763 precipitation likely to drive below-average agricultural and livestock production in 2021, 2021.
- 764 Funk, C., Peterson, P., Landsfeld, M., Pedreros, D., Verdin, J., Shukla, S., Husak, G., Rowland, J.,
765 Harrison, L., Hoell, A., and Michaelsen, J.: The climate hazards infrared precipitation with stations--
766 a new environmental record for monitoring extremes., The climate hazards infrared precipitation
767 with stations—a new environmental record for monitoring extremes, *Sci Data*, 2, 2, 150066–
768 150066, <https://doi.org/10.1038/sdata.2015.66>, 10.1038/sdata.2015.66, 2015.
- 769 Funk, C. C., Peterson, P., Huffman, G. J., Landsfeld, M. F., Peters-Lidard, C., Davenport, F.,
770 Shukla, S., Peterson, S., Pedreros, D. H., Ruane, A. C., Mutter, C., Turner, W., Harrison, L.,
771 Sonnier, A., Way-Henthorne, J., and Husak, G. J.: Introducing and Evaluating the Climate Hazards
772 Center IMERG with Stations (CHIMES): Timely Station-Enhanced Integrated Multisatellite
773 Retrievals for Global Precipitation Measurement, 103, E429–E454, [https://doi.org/10.1175/BAMS-](https://doi.org/10.1175/BAMS-D-20-0245.1)
774 [D-20-0245.1](https://doi.org/10.1175/BAMS-D-20-0245.1), 2022.
- 775 Gadelha, A. N., Coelho, V. H. R., Xavier, A. C., Barbosa, L. R., Melo, D. C. D., Xuan, Y.,
776 Huffman, G. J., Petersen, W. A., and Almeida, C. das N.: Grid box-level evaluation of IMERG over
777 Brazil at various space and time scales, *Atmospheric Research*, 218, 231–244,
778 <https://doi.org/10.1016/j.atmosres.2018.12.001>, 2019.
- 779 Gelaro, R., McCarty, W., Suárez, M. J., Todling, R., Molod, A., Takacs, L., Randles, C. A.,
780 Darmenov, A., Bosilovich, M. G., Reichle, R., Wargan, K., Coy, L., Cullather, R., Draper, C.,
781 Akella, S., Buchard, V., Conaty, A., da Silva, A. M., Gu, W., Kim, G.-K., Koster, R., Lucchesi, R.,
782 Merkova, D., Nielsen, J. E., Partyka, G., Pawson, S., Putman, W., Rienecker, M., Schubert, S. D.,
783 Sienkiewicz, M., and Zhao, B.: The Modern-Era Retrospective Analysis for Research and
784 Applications, Version 2 (MERRA-2), *J. Climate*, 30, 5419–5454, [https://doi.org/10.1175/JCLI-D-](https://doi.org/10.1175/JCLI-D-16-0758.1)
785 [16-0758.1](https://doi.org/10.1175/JCLI-D-16-0758.1), 2017.
- 786 GEOGLAM: Early Warning Crop Monitor February 2018,
787 https://cropmonitor.org/documents/EWCM/reports/EarlyWarning_CropMonitor_201802.pdf,
788 2018a.
- 789 GEOGLAM: Early Warning Crop Monitor March 2018,
790 https://cropmonitor.org/documents/EWCM/reports/EarlyWarning_CropMonitor_201802.pdf,
791 2018b.
- 792 Ghatak, D., Zaitchik, B., Kumar, S., Matin, M. A., Bajracharya, B., Hain, C., and Anderson, M.:
793 Influence of Precipitation Forcing Uncertainty on Hydrological Simulations with the NASA South
794 Asia Land Data Assimilation System, *Hydrology*, 5, 57, <https://doi.org/10.3390/hydrology5040057>,
795 2018.

- 796 Grace, K. and Davenport, F.: Climate variability and health in extremely vulnerable communities:
797 investigating variations in surface water conditions and food security in the West African Sahel,
798 *Population & Environment*, 42, 553–577, <https://doi.org/10.1007/s11111-021-00375-9>, 2021.
- 799 Gutman, G. and Ignatov, A.: The derivation of the green vegetation fraction from NOAA/AVHRR
800 data for use in numerical weather prediction models, *International Journal of Remote Sensing*, 19,
801 1533–1543, <https://doi.org/10.1080/014311698215333>, 1998.
- 802 Hall, D. and Riggs, G.: MODIS/Terra Snow Cover Daily L3 Global 500m SIN Grid version 6,
803 <https://doi.org/10.5067/MODIS/MOD10A1.006>, 2016.
- 804 Hengl, T., Jesus, J. M. de, Heuvelink, G. B. M., Gonzalez, M. R., Kilibarda, M., Blagotić, A.,
805 Shangguan, W., Wright, M. N., Geng, X., Bauer-Marschallinger, B., Guevara, M. A., Vargas, R.,
806 MacMillan, R. A., Batjes, N. H., Leenaars, J. G. B., Ribeiro, E., Wheeler, I., Mantel, S., and
807 Kempen, B.: SoilGrids250m: Global gridded soil information based on machine learning, *PLOS*
808 *ONE*, 12, e0169748, <https://doi.org/10.1371/journal.pone.0169748>, 2017.
- 809 Hewitt, C., Mason, S., and Walland, D.: The Global Framework for Climate Services, *Nature Clim*
810 *Change*, 2, 831–832, <https://doi.org/10.1038/nclimate1745>, 2012.
- 811 Hoell, A., Funk, C., and Barlow, M.: The Forcing of Southwestern Asia Teleconnections by Low-
812 Frequency Sea Surface Temperature Variability during Boreal Winter, *J. Climate*, 28, 1511–1526,
813 <https://doi.org/10.1175/JCLI-D-14-00344.1>, 2015.
- 814 Hoell, A., Barlow, M., Cannon, F., and Xu, T.: Oceanic Origins of Historical Southwest Asia
815 Precipitation During the Boreal Cold Season, *J. Climate*, 30, 2885–2903,
816 <https://doi.org/10.1175/JCLI-D-16-0519.1>, 2017.
- 817 Hoell, A., Cannon, F., and Barlow, M.: Middle East and Southwest Asia Daily Precipitation
818 Characteristics Associated with the Madden–Julian Oscillation during Boreal Winter, *J. Climate*, 31,
819 8843–8860, <https://doi.org/10.1175/JCLI-D-18-0059.1>, 2018.
- 820 Hoell, A., Eischeid, J., Barlow, M., and McNally, A.: Characteristics, precursors, and potential
821 predictability of Amu Darya Drought in an Earth system model large ensemble, *Clim Dyn*, 55,
822 2185–2206, <https://doi.org/10.1007/s00382-020-05381-5>, 2020.
- 823 Huffman, G. J., Bolvin, D. T., Braithwaite, D., Hsu, K.-L., Joyce, R. J., Kidd, C., Nelkin, E. J.,
824 Sorooshian, S., Stocker, E. F., Tan, J., Wolff, D. B., and Xie, P.: Integrated Multi-satellite Retrievals
825 for the Global Precipitation Measurement (GPM) Mission (IMERG), in: *Satellite Precipitation*
826 *Measurement: Volume 1*, edited by: Levizzani, V., Kidd, C., Kirschbaum, D. B., Kummerow, C. D.,
827 Nakamura, K., and Turk, F. J., Springer International Publishing, Cham, 343–353,
828 https://doi.org/10.1007/978-3-030-24568-9_19, 2020.

- 829 Immerzeel, W. W., Wanders, N., Lutz, A. F., Shea, J. M., and Bierkens, M. F. P.: Reconciling high-
830 altitude precipitation in the upper Indus basin with glacier mass balances and runoff, *Hydrol. Earth*
831 *Syst. Sci.*, 19, 4673–4687, <https://doi.org/10.5194/hess-19-4673-2015>, 2015.
- 832 Jacob, J. and Slinski, K.: GES DISC Dataset: FLDAS Noah Land Surface Model L4 Central Asia
833 Daily 0.01 x 0.01 degree (FLDAS_NOAH001_G_CA_D 001),
834 <https://doi.org/10.5067/VQ4CD3Y9YC0R>, 2021.
- 835 Jung, H. C., Getirana, A., Policelli, F., McNally, A., Arsenault, K. R., Kumar, S., Tadesse, T., and
836 Peters-Lidard, C. D.: Upper Blue Nile basin water budget from a multi-model perspective, *Journal*
837 *of Hydrology*, 555, 535–546, <https://doi.org/10.1016/j.jhydrol.2017.10.040>, 2017.
- 838 Jung, H. C., Getirana, A., Arsenault, K. R., Holmes, T. R. H., and McNally, A.: Uncertainties in
839 Evapotranspiration Estimates over West Africa, *Remote Sensing*, 11, 892,
840 <https://doi.org/10.3390/rs11080892>, 2019.
- 841 Kato, H. and Rodell, M.: Sensitivity of Land Surface Simulations to Model Physics, Land
842 Characteristics, and Forcings, at Four CEOP Sites, *Journal of the Meteorological Society of Japan.*
843 *Ser. II, Volume 85A*, 187–204, <https://doi.org/10.2151/jmsj.85A.187>, 2007.
- 844 Kirschbaum, D. B., Huffman, G. J., Adler, R. F., Braun, S., Garrett, K., Jones, E., McNally, A.,
845 Skofronick-Jackson, G., Stocker, E., Wu, H., and Zaitchik, B. F.: NASA’s Remotely Sensed
846 Precipitation: A Reservoir for Applications Users, *Bull. Amer. Meteor. Soc.*, 98, 1169–1184,
847 <https://doi.org/10.1175/BAMS-D-15-00296.1>, 2016.
- 848 Kumar, S. V., Peters-Lidard, C. D., Tian, Y., Houser, P. R., Geiger, J., Olden, S., Lighty, L.,
849 Eastman, J. L., Doty, B., Dirmeyer, P., Adams, J., Mitchell, K., Wood, E. F., and Sheffield, J.: Land
850 information system: An interoperable framework for high resolution land surface modeling,
851 *Environmental Modelling & Software*, 21, 1402–1415,
852 <https://doi.org/10.1016/j.envsoft.2005.07.004>, 2006.
- 853 Kumar, S. V., Peters-Lidard, C. D., Santanello, J., Harrison, K., Liu, Y., and Shaw, M.: Land
854 surface Verification Toolkit (LVT) – a generalized framework for land surface model evaluation,
855 *Geosci. Model Dev.*, 5, 869–886, <https://doi.org/10.5194/gmd-5-869-2012>, 2012.
- 856 Kumar, S. V., Peters-Lidard, C. D., Mocko, D., and Tian, Y.: Multiscale Evaluation of the
857 Improvements in Surface Snow Simulation through Terrain Adjustments to Radiation, *Journal of*
858 *Hydrometeorology*, 14, 220–232, <https://doi.org/10.1175/JHM-D-12-046.1>, 2013.
- 859 Ma, Z., Xu, J., Zhu, S., Yang, J., Tang, G., Yang, Y., Shi, Z., and Hong, Y.: AIMERG: a new Asian
860 precipitation dataset (0.1°/half-hourly, 2000–2015) by calibrating the GPM-era IMERG at a daily
861 scale using APHRODITE, *Earth Syst. Sci. Data*, 12, 1525–1544, [https://doi.org/10.5194/essd-12-](https://doi.org/10.5194/essd-12-1525-2020)
862 [1525-2020](https://doi.org/10.5194/essd-12-1525-2020), 2020.

- 863 Manz, B., Páez-Bimos, S., Horna, N., Buytaert, W., Ochoa-Tocachi, B., Lavado-Casimiro, W., and
864 Willems, B.: Comparative Ground Validation of IMERG and TMPA at Variable Spatiotemporal
865 Scales in the Tropical Andes, *Journal of Hydrometeorology*, 18, 2469–2489,
866 <https://doi.org/10.1175/JHM-D-16-0277.1>, 2017.
- 867 McNally, A.: GES DISC Dataset: FLDAS Noah Land Surface Model L4 Global Monthly 0.1 x 0.1
868 degree (MERRA-2 and CHIRPS) (FLDAS_NOAH01_C_GL_M 001), 2018.
- 869 McNally, A., Husak, G. J., Brown, M., Carroll, M., Funk, C., Yatheendradas, S., Arsenault, K.,
870 Peters-Lidard, C., and Verdin, J. P.: Calculating Crop Water Requirement Satisfaction in the West
871 Africa Sahel with Remotely Sensed Soil Moisture, *J. Hydrometeor.*, 16, 295–305,
872 <https://doi.org/10.1175/JHM-D-14-0049.1>, 2015.
- 873 McNally, A., Shukla, S., Arsenault, K. R., Wang, S., Peters-Lidard, C. D., and Verdin, J. P.:
874 Evaluating ESA CCI soil moisture in East Africa, *International Journal of Applied Earth
875 Observation and Geoinformation*, 48, 96–109, <https://doi.org/10.1016/j.jag.2016.01.001>, 2016.
- 876 McNally, A., Arsenault, K., Kumar, S., Shukla, S., Peterson, P., Wang, S., Funk, C., Peters-lidard,
877 C. D., and Verdin, J. P.: A land data assimilation system for sub-Saharan Africa food and water
878 security applications, *Scientific Data*, 4, 170012, <http://dx.doi.org/10.1038/sdata.2017.12>, 2017.
- 879 McNally, A., McCartney, S., Ruane, A. C., Mladenova, I. E., Whitcraft, A. K., Becker-Reshef, I.,
880 Bolten, J. D., Peters-Lidard, C. D., Rosenzweig, C., and Uz, S. S.: Hydrologic and Agricultural
881 Earth Observations and Modeling for the Water-Food Nexus, *Front. Environ. Sci.*, 7,
882 <https://doi.org/10.3389/fenvs.2019.00023>, 2019.
- 883 Miller, J., Barlage, M., Zeng, X., Wei, H., Mitchell, K., and Tarpley, D.: Sensitivity of the
884 NCEP/Noah land surface model to the MODIS green vegetation fraction data set, *Geophys. Res.
885 Lett.*, 33, <https://doi.org/10.1029/2006GL026636>, 2006.
- 886 Molteni, F., Buizza, R., Palmer, T. N., and Petroliagis, T.: The ECMWF Ensemble Prediction
887 System: Methodology and validation, *Q J R Meteorol Soc*, 122, 73–119,
888 <https://doi.org/10.1002/qj.49712252905>, 1996.
- 889 NASA Earth Observatory: Record Low Snowpack in Afghanistan, NASA Earth Observatory, 2018.
- 890 NASA JPL: NASA Shuttle Radar Topography Mission Global 30 arc second [Data set]. NASA
891 EOSDIS Land Processes DAAC, NASA EOSDIS Land Processes DAAC, NASA EOSDIS Land
892 Processes DAAC., 2013.
- 893 Nazemosadat, M. J. and Ghaedamini, H.: On the Relationships between the Madden–Julian
894 Oscillation and Precipitation Variability in Southern Iran and the Arabian Peninsula: Atmospheric
895 Circulation Analysis, 23, 887–904, <https://doi.org/10.1175/2009JCLI2141.1>, 2010.

- 896 NCAR Research Applications Library: <https://ral.ucar.edu/solutions/products/unified-noah-lsm>, last
897 access: 12 November 2021.
- 898 Niu, G.-Y., Yang, Z.-L., Mitchell, K. E., Chen, F., Ek, M. B., Barlage, M., Kumar, A., Manning, K.,
899 Niyogi, D., Rosero, E., Tewari, M., and Xia, Y.: The community Noah land surface model with
900 multiparameterization options (Noah-MP): 1. Model description and evaluation with local-scale
901 measurements, *JGR: Atmospheres*, 116, <https://doi.org/10.1029/2010JD015139>, 2011.
- 902 NOAA: [https://www.climate.gov/news-features/blogs/enso/september-enso-update-la-ni%C3%B1a-](https://www.climate.gov/news-features/blogs/enso/september-enso-update-la-ni%C3%B1a-watch)
903 [watch](https://www.climate.gov/news-features/blogs/enso/september-enso-update-la-ni%C3%B1a-watch), last access: 12 September 2017.
- 904 NOAA CPC ENSO Cold & Warm Episodes by Season:
905 https://origin.cpc.ncep.noaa.gov/products/analysis_monitoring/ensostuff/ONI_v5.php, last access:
906 29 July 2021.
- 907 Oki, T. and Kanae, S.: Global Hydrological Cycles and World Water Resources, *Science*, 313,
908 1068–1072, <https://doi.org/10.1126/science.1128845>, 2006.
- 909 Pervez, S., McNally, A., Arsenault, K., Budde, M., and Rowland, J.: Vegetation Monitoring
910 Optimization With Normalized Difference Vegetation Index and Evapotranspiration Using Remote
911 Sensing Measurements and Land Surface Models Over East Africa, *Frontiers in Climate*, 3, 1,
912 <https://doi.org/10.3389/fclim.2021.589981>, 2021.
- 913 Peters-Lidard, C. D., Houser, P. R., Tian, Y., Kumar, S. V., Geiger, J., Olden, S., Lighty, L., Doty,
914 B., Dirmeyer, P., Adams, J., Mitchell, K., Wood, E. F., and Sheffield, J.: High-performance Earth
915 system modeling with NASA/GSFC’s Land Information System, *Innovations Syst Softw Eng*, 3,
916 157–165, <https://doi.org/10.1007/s11334-007-0028-x>, 2007.
- 917 Qamer, F. M., Tadesse, T., Matin, M., Ellenburg, W. L., and Zaitchik, B.: Earth Observation and
918 Climate Services for Food Security and Agricultural Decision Making in South and Southeast Asia,
919 *Bull Am Meteorol Soc*, 100, ES171–ES174, <https://doi.org/10.1175/BAMS-D-18-0342.1>, 2019.
- 920 Rana, S., Renwick, J., McGregor, J., and Singh, A.: Seasonal Prediction of Winter Precipitation
921 Anomalies over Central Southwest Asia: A Canonical Correlation Analysis Approach, *J. Climate*,
922 31, 727–741, <https://doi.org/10.1175/JCLI-D-17-0131.1>, 2018.
- 923 Reynolds, C. A., Jackson, T. J., and Rawls, W. J.: Estimating soil water-holding capacities by
924 linking the Food and Agriculture Organization Soil map of the world with global pedon databases
925 and continuous pedotransfer functions, *Water Resources Research*, 36, 3653–3662,
926 <https://doi.org/10.1029/2000WR900130>, 2000.

- 927 Sarmiento, D. P., Slinski, K., McNally, A., Funk, C., Peterson, P., and Peters-Lidard, C. D.: Daily
928 precipitation frequency distributions impacts on land-surface simulations of CONUS, *Front. Water*,
929 0, <https://doi.org/10.3389/frwa.2021.640736>, 2021.
- 930 Schiemann, R., Lüthi, D., Vidale, P. L., and Schär, C.: The precipitation climate of Central Asia—
931 intercomparison of observational and numerical data sources in a remote semiarid region, *Royal*
932 *Meteorological Society*, 28, 295–314, <https://doi.org/10.1002/joc.1532>, 2008.
- 933 Schneider, U., Finger, P., Meyer-Christoffer, A., Rustemeier, E., Ziese, M., and Becker, A.:
934 Evaluating the Hydrological Cycle over Land Using the Newly-Corrected Precipitation Climatology
935 from the Global Precipitation Climatology Centre (GPCC), 8, 52,
936 <https://doi.org/10.3390/atmos8030052>, 2017.
- 937 Senay, G. B., Bohms, S., Singh, R. K., Gowda, P. H., Velpuri, N. M., Alemu, H., and Verdin, J. P.:
938 Operational Evapotranspiration Mapping Using Remote Sensing and Weather Datasets: A New
939 Parameterization for the SSEB Approach, *J Am Water Resour Assoc*, 49, 577–591,
940 <https://doi.org/10.1111/jawr.12057>, 2013.
- 941 Shukla, S., Arsenault, K. R., Hazra, A., Peters-Lidard, C., Koster, R. D., Davenport, F., Magadzire,
942 T., Funk, C., Kumar, S., McNally, A., Getirana, A., Husak, G., Zaitchik, B., Verdin, J., Nsadisa, F.
943 D., and Becker-Reshef, I.: Improving early warning of drought-driven food insecurity in southern
944 Africa using operational hydrological monitoring and forecasting products, *Nat. Hazards Earth Syst.*
945 *Sci.*, 20, 1187–1201, <https://doi.org/10.5194/nhess-20-1187-2020>, 2020.
- 946 Shukla, S., Landsfeld, M., Anthony, M., Budde, M., Husak, G. J., Rowland, J., and Funk, C.:
947 Enhancing the Application of Earth Observations for Improved Environmental Decision-Making
948 Using the Early Warning eXplorer (EWX), *Frontiers in Climate*, 2, 34,
949 <https://doi.org/10.3389/fclim.2020.583509>, 2021.
- 950 Tabar, M., Gluck, J., Goyal, A., Jiang, F., Morr, D., Kehs, A., Lee, D., Hughes, D. P., and Yadav,
951 A.: A PLAN for Tackling the Locust Crisis in East Africa: Harnessing Spatiotemporal Deep Models
952 for Locust Movement Forecasting, in: *Proceedings of the 27th ACM SIGKDD Conference on*
953 *Knowledge Discovery & Data Mining*, New York, NY, USA, 3595–3604,
954 <https://doi.org/10.1145/3447548.3467184>, 2021.
- 955 Tan, J., Petersen, W. A., and Tokay, A.: A Novel Approach to Identify Sources of Errors in IMERG
956 for GPM Ground Validation, *Journal of Hydrometeorology*, 17, 2477–2491,
957 <https://doi.org/10.1175/JHM-D-16-0079.1>, 2016.
- 958 UNICEF: 500,000 children affected by drought in Afghanistan – UNICEF,
959 <https://www.unicef.org/press-releases/500000-children-affected-drought-afghanistan-unicef>, 2018.

- 960 USGS Knowledge Base:
961 <https://earlywarning.usgs.gov/fews/searchkb/Asia/Central%20Asia/Afghanistan>, last access: 12
962 November 2021.
- 963 Vincent, K., Daly, M., Scannell, C., and Leathes, B.: What can climate services learn from theory
964 and practice of co-production?, *Climate Services*, 12, 48–58,
965 <https://doi.org/10.1016/j.cliser.2018.11.001>, 2018.
- 966 Xie, P. and Arkin, P. A.: Analyses of Global Monthly Precipitation Using Gauge Observations,
967 Satellite Estimates, and Numerical Model Predictions, *Journal of Climate*, 9, 840–858,
968 [https://doi.org/10.1175/1520-0442\(1996\)009<0840:AOGMPU>2.0.CO;2](https://doi.org/10.1175/1520-0442(1996)009<0840:AOGMPU>2.0.CO;2), 1996.
- 969 Yatagai, A., Kamiguchi, K., Arakawa, O., Hamada, A., Yasutomi, N., and Kitoh, A.: APHRODITE:
970 Constructing a Long-Term Daily Gridded Precipitation Dataset for Asia Based on a Dense Network
971 of Rain Gauges, *Bull Am Meteorol Soc*, 93, 1401–1415, [https://doi.org/10.1175/BAMS-D-11-](https://doi.org/10.1175/BAMS-D-11-00122.1)
972 [00122.1](https://doi.org/10.1175/BAMS-D-11-00122.1), 2012.
- 973 Yoon, Y., Kumar, S. V., Forman, B. A., Zaitchik, B. F., Kwon, Y., Qian, Y., Rupper, S., Maggioni,
974 V., Houser, P., Kirschbaum, D., Richey, A., Arendt, A., Mocko, D., Jacob, J., Bhanja, S., and
975 Mukherjee, A.: Evaluating the Uncertainty of Terrestrial Water Budget Components Over High
976 Mountain Asia, *Frontiers in Earth Science*, 7, 120, <https://doi.org/10.3389/feart.2019.00120>, 2019.

977